Weierstrass Institute for
Applied Analysis and Stochastics

Mathematical opportunities and challenges in sustainable energies

Barbara Wagner

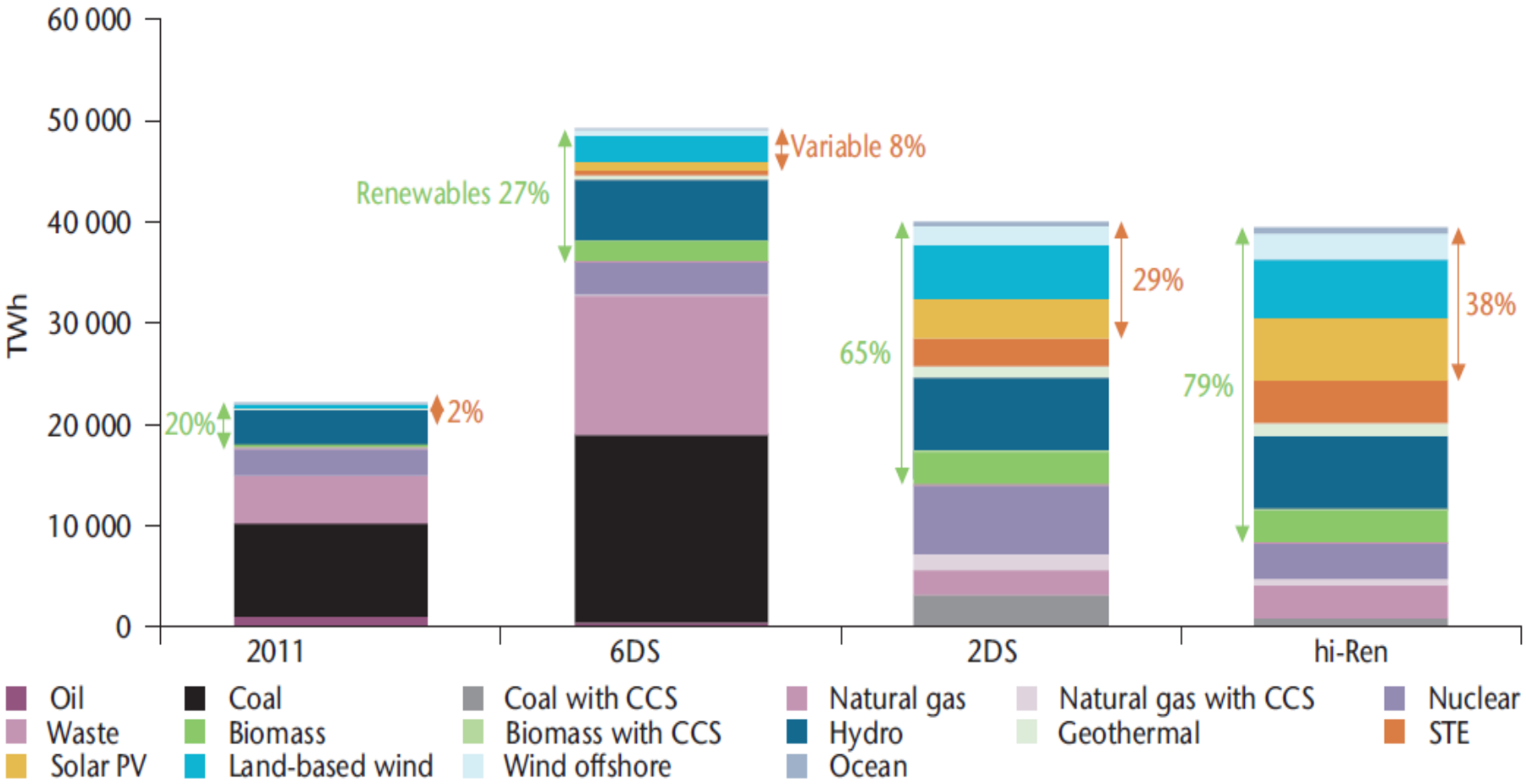

IEA Energy Technology Perspectives 2014b

Photovoltaics, Solar Thermal Energy, Concentrated Solar Power, ...

Photo: Harvey Georges/Corbis

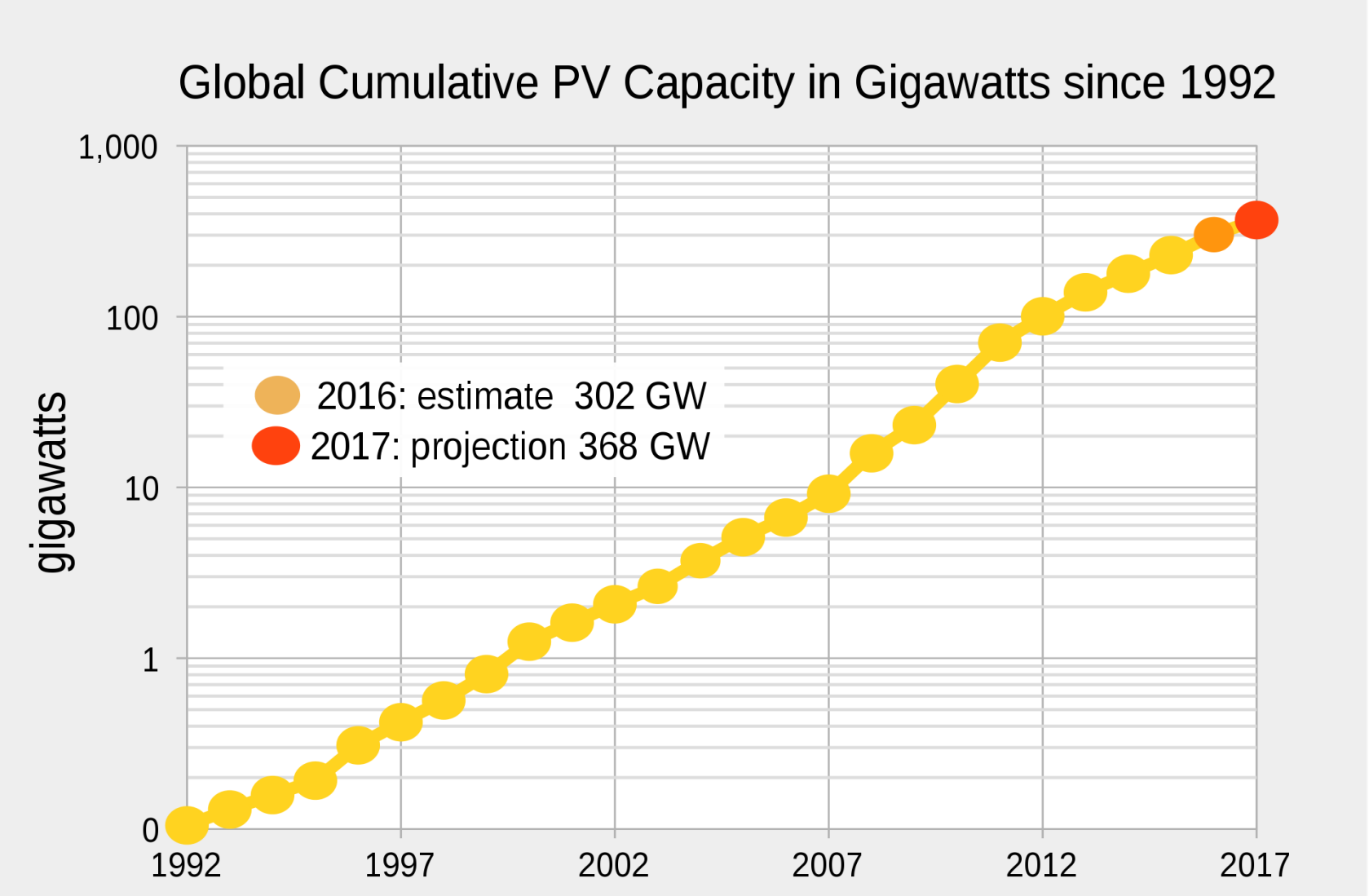

Global Market Outlook for Solar Power 2014, 2015, 2016

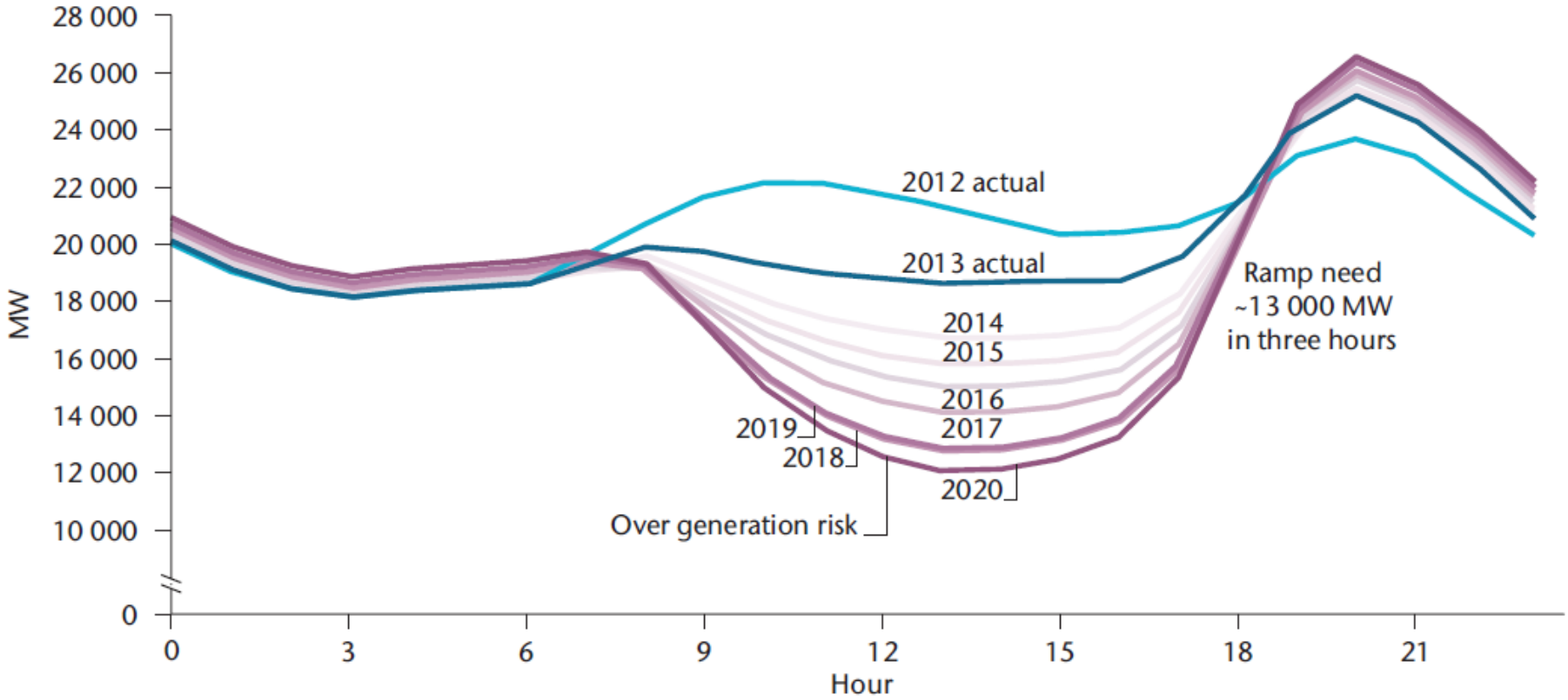

Source: California ISO (Independent System Operator) (2013), *What the Duck Chart Tells Us About Managing a Green Grid*, Fast Facts, Folsom, CA, accessed 4 June 2014.

- **Storage:** large-scale stationary battery systems, solar fuels, hydrogen, ...
- **Networks:** prosumers (household solar power systems, electric vehicle batteries, ...)

- **Storage:** large-scale stationary battery systems, solar fuels, hydrogen, ...
- **Networks:** prosumers (household solar power systems, electric vehicle batteries, ...)

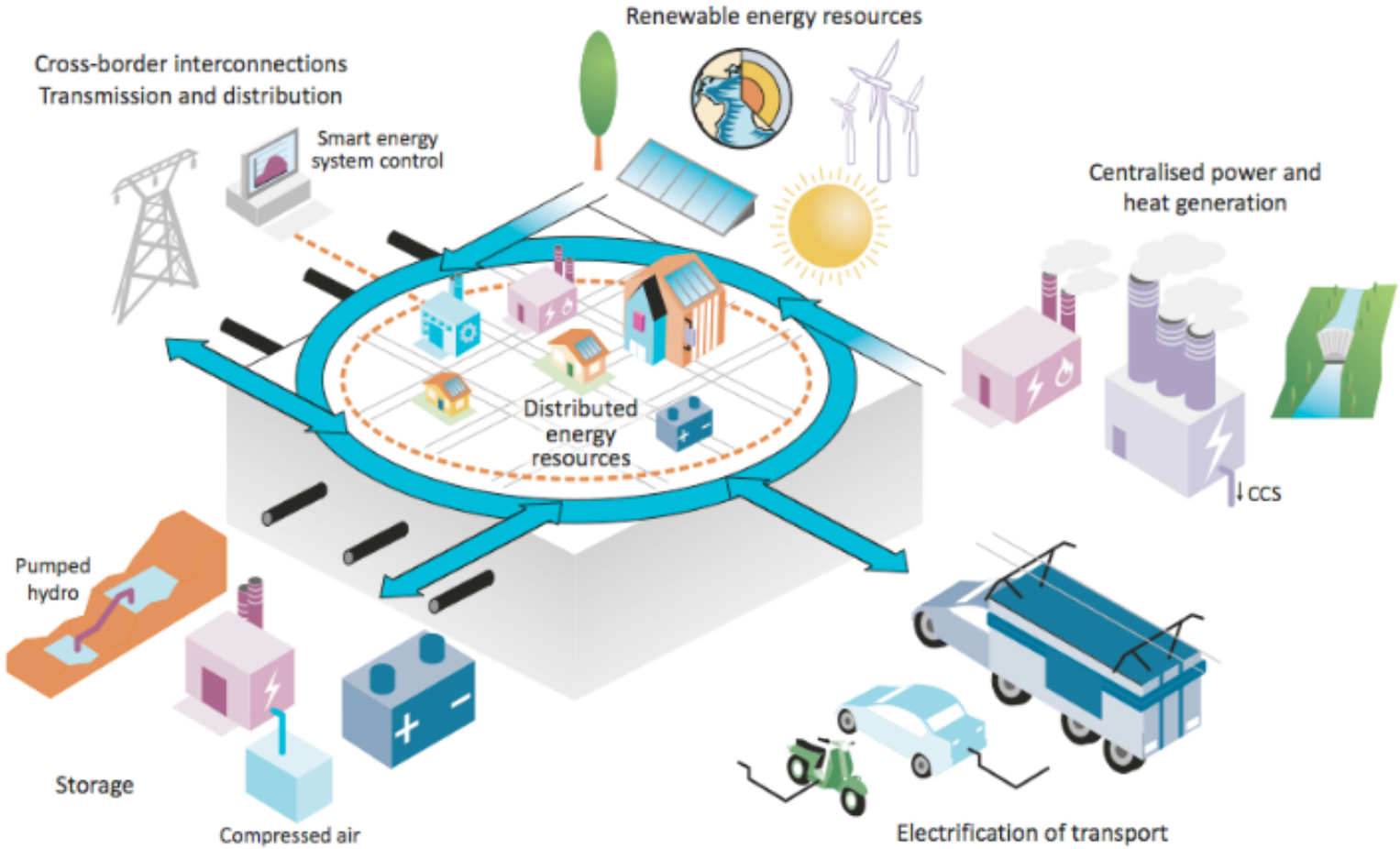

Note: CCS = carbon capture and storage.

Source: Reprinted from IEA (2014b), *Energy Technology Perspectives*.

1 Photovoltaics

2 Case studies: Microstructure control

3 Rechargeable batteries

SOLAR CELL

- Basic principle: **pn-junction**
- p-layer and n-layer brought together
  - ⇒ **Depletion layer**
  - ⇒ electric field
- Photon hits silicon atom ⇒ electron excited from valence to conduction band
- electron “sees” DL ⇒ electrode

Heart of the solar cell

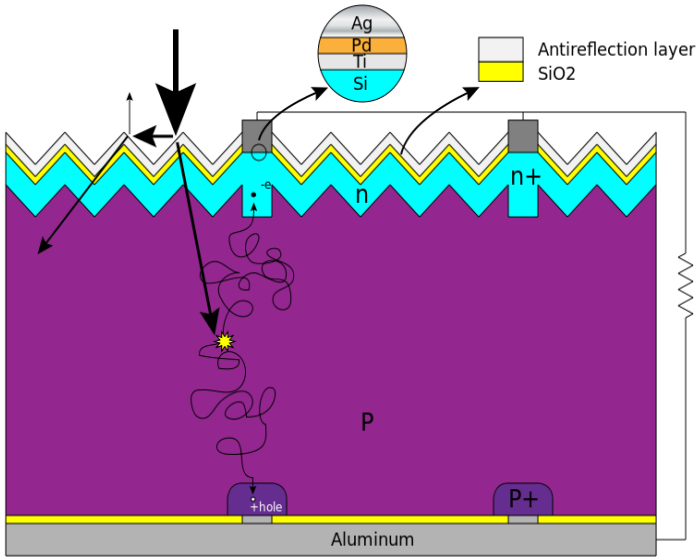

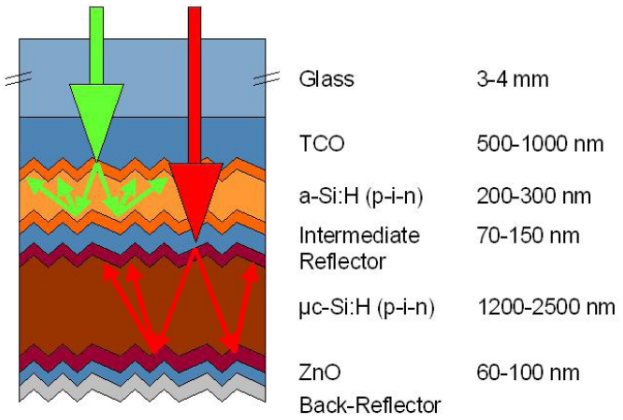

SOLAR CELL

- Basic principle: **pn-junction**
- p-layer and n-layer brought together
  - ⇒ **Depletion layer**
  - ⇒ electric field
- Photon hits silicon atom ⇒ electron excited from valence to conduction band
- electron “sees” DL ⇒ electrode

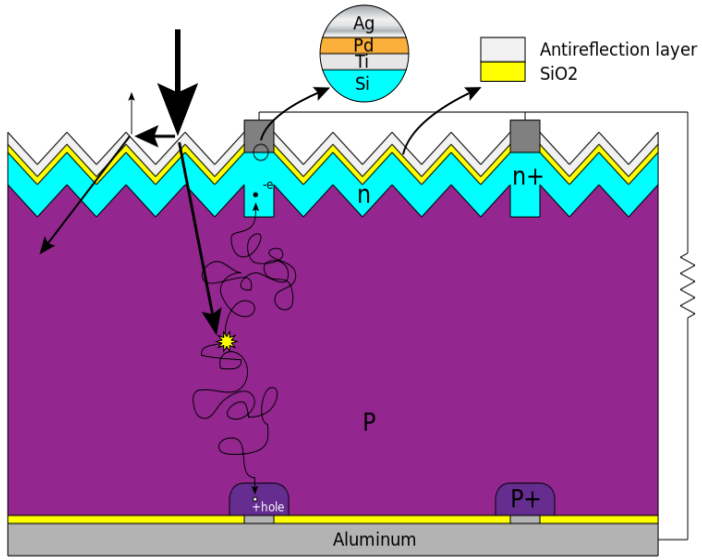

Heart of the solar cell

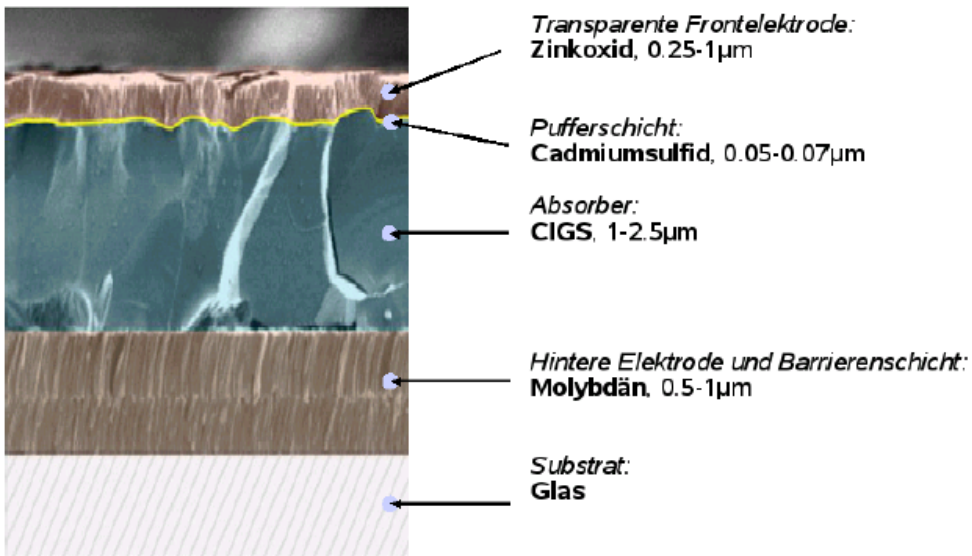

SOLAR CELL

- Basic principle: **pn-junction**
- p-layer and n-layer brought together
  - ⇒ **Depletion layer**
  - ⇒ electric field
- Photon hits silicon atom ⇒ electron excited from valence to conduction band
- electron “sees” DL ⇒ electrode

Heart of the solar cell

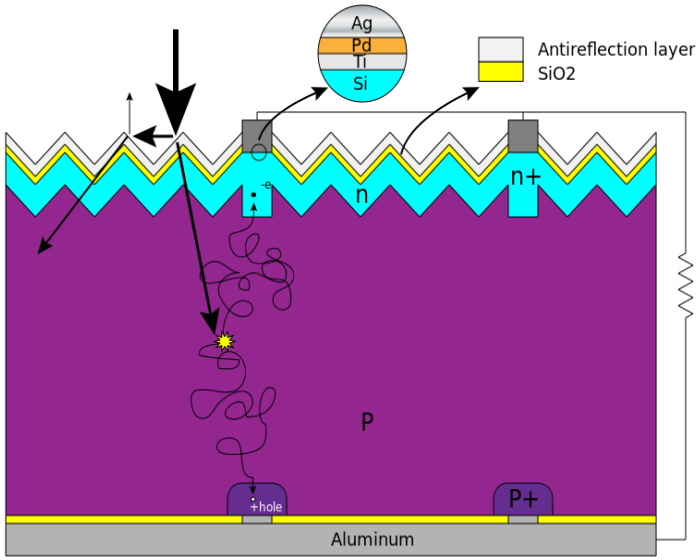

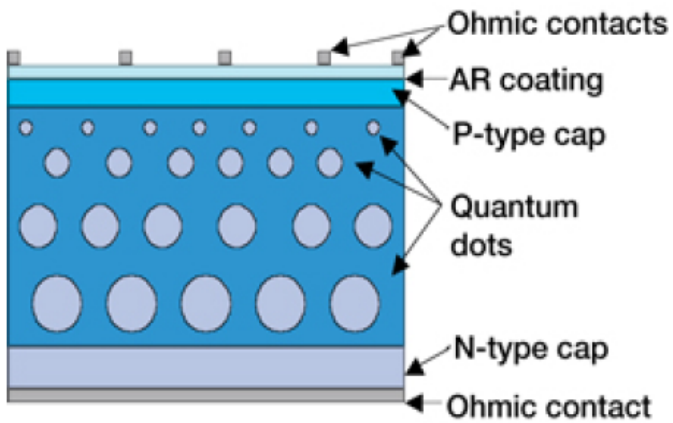

S. M. Shauddin, Energy and Power (2013)

SOLAR CELL

- Basic principle: **pn-junction**
- p-layer and n-layer brought together
  - ⇒ **Depletion layer**
  - ⇒ electric field
- Photon hits silicon atom ⇒ electron excited from valence to conduction band
- electron “sees” DL ⇒ electrode

Heart of the solar cell

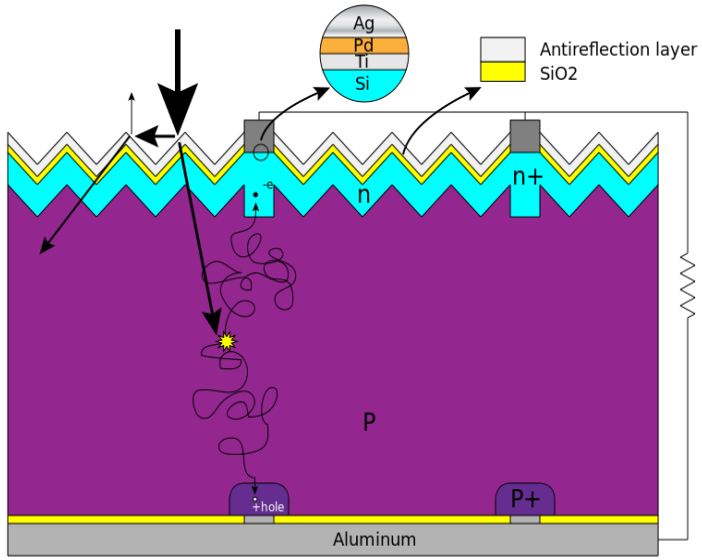

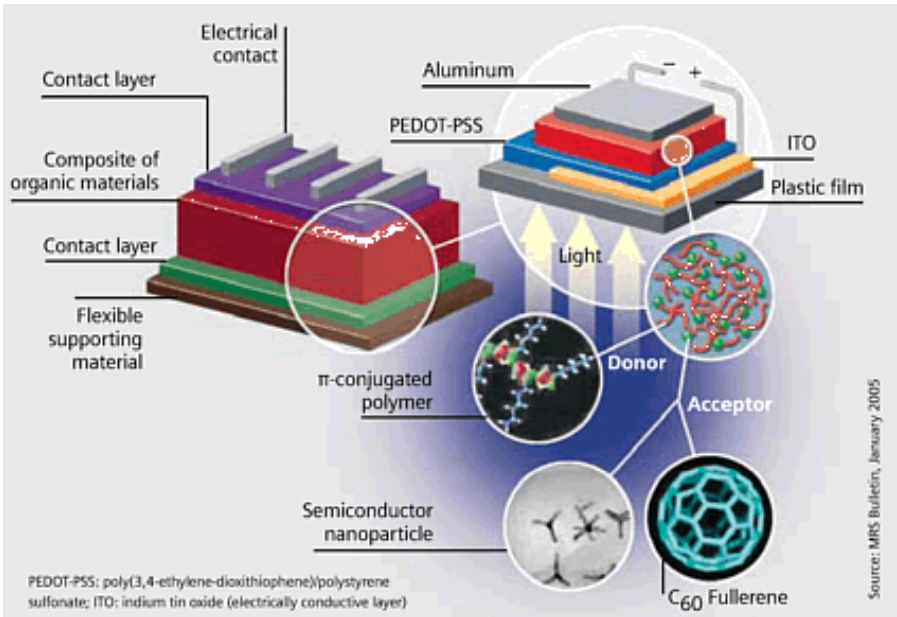

SOLAR CELL

- Basic principle: **pn-junction**
- p-layer and n-layer brought together
  - ⇒ **Depletion layer**
  - ⇒ electric field
- Photon hits silicon atom ⇒ electron excited from valence to conduction band
- electron “sees” DL ⇒ electrode

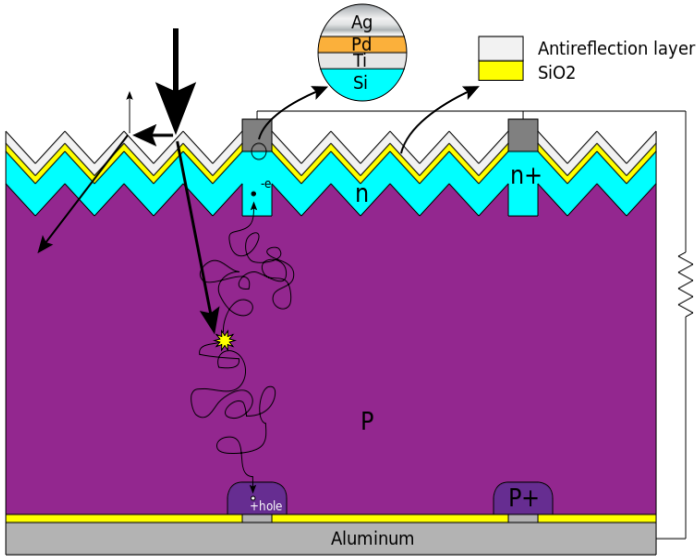

Heart of the solar cell

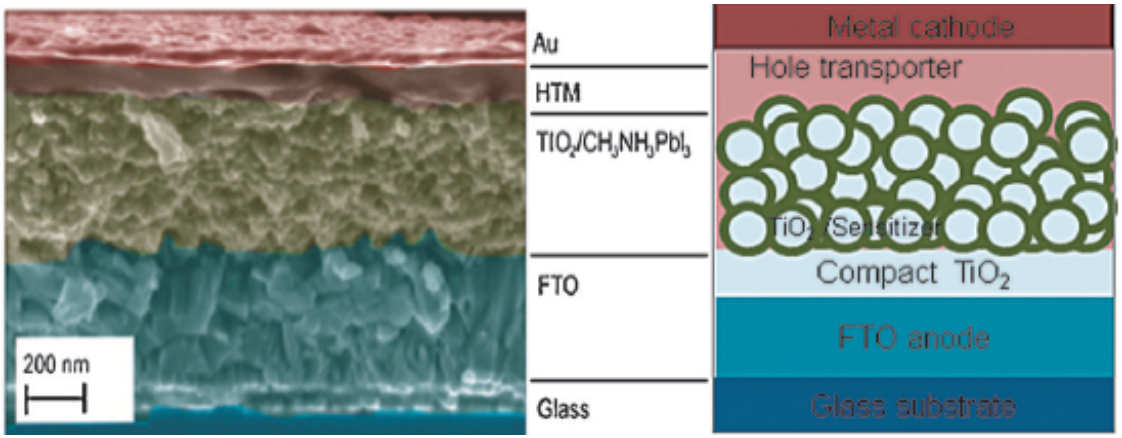

Burschka et al., Nature (2013)

Best Research-Cell Efficiencies

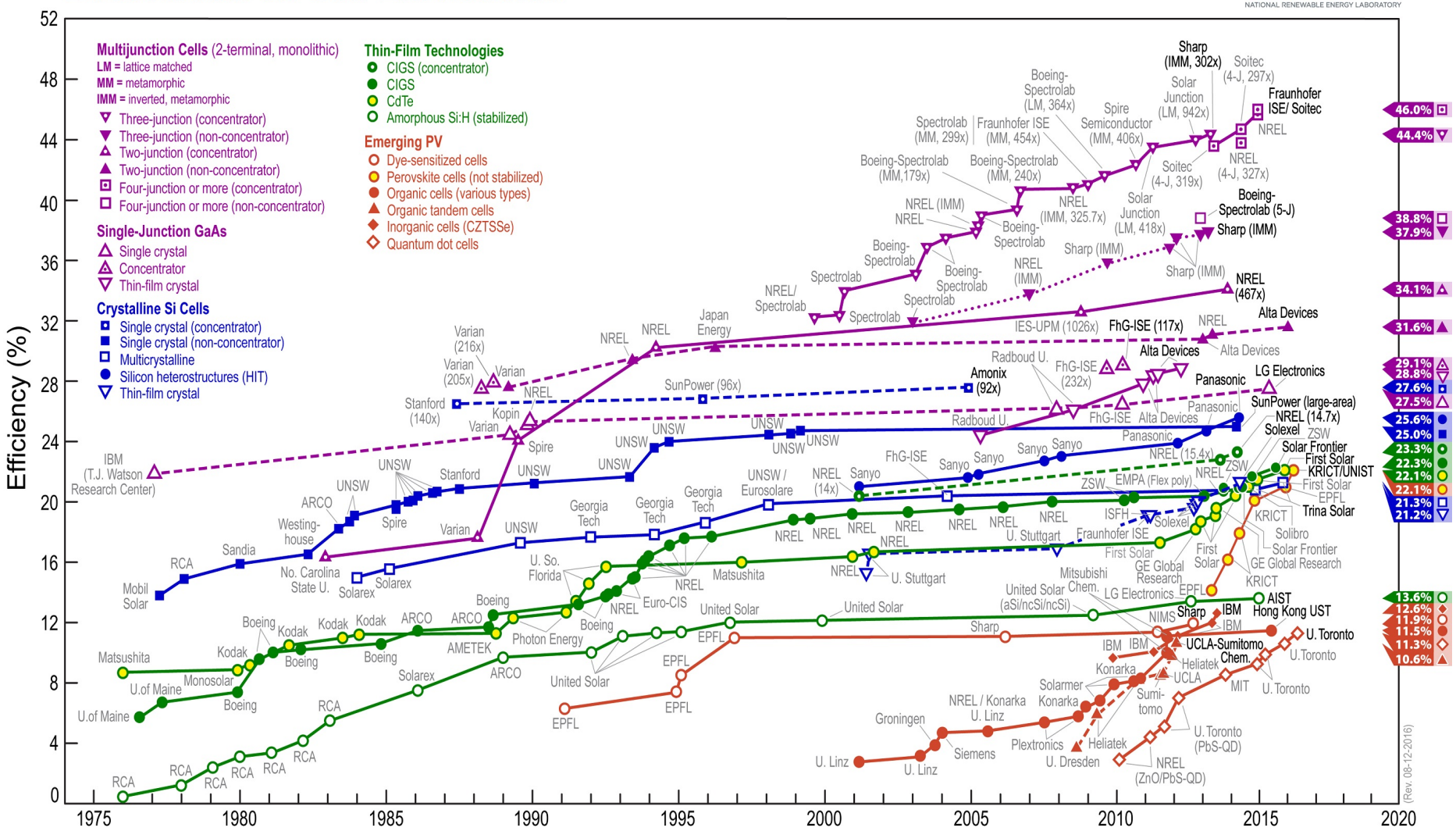

Best Research-Cell Efficiencies

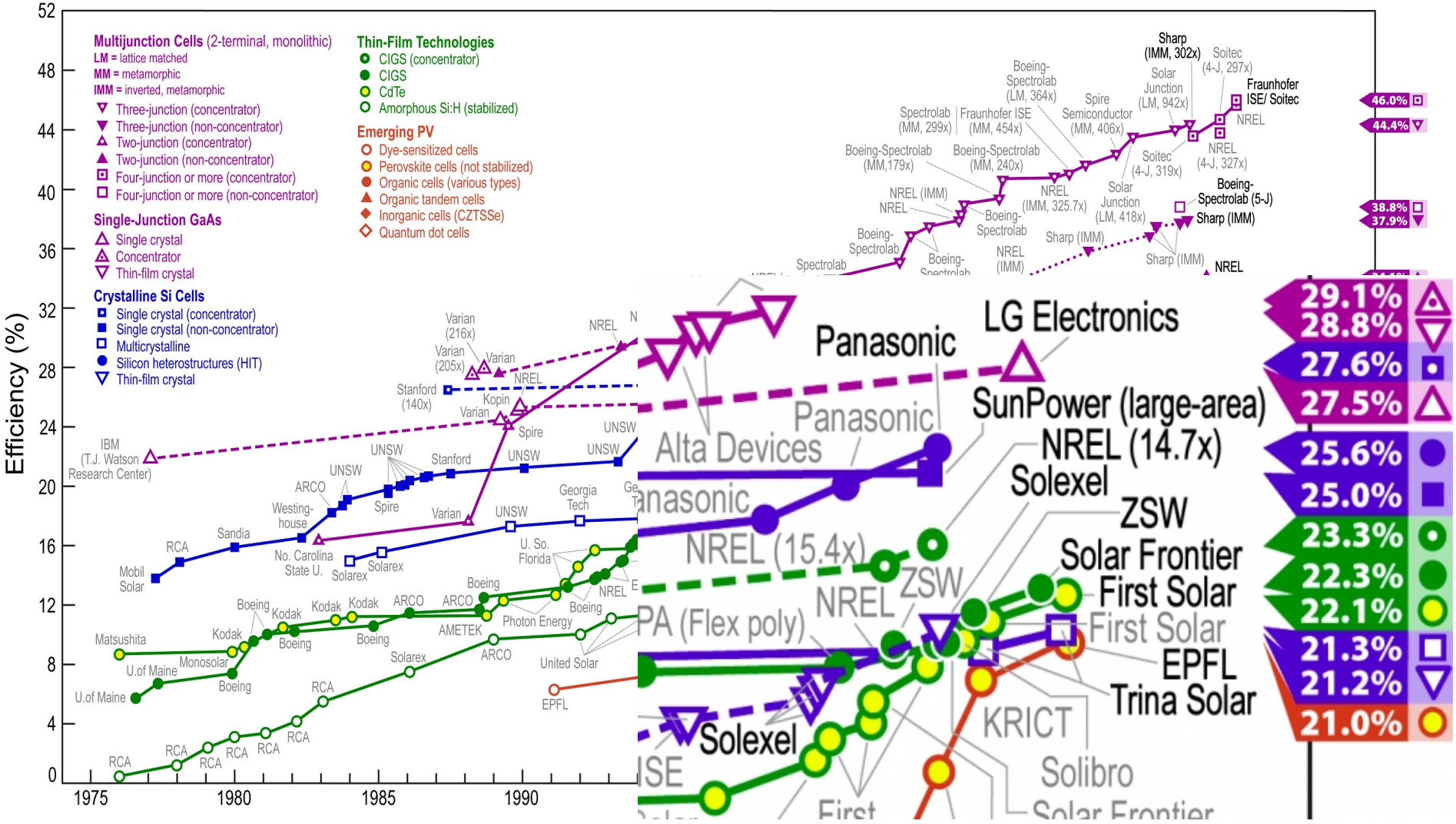

- **2011:** Helmholtz-NREL Solar Energy Initative collaborate on

  "...materials and technology that will form the basis of solar cells and solar fuels in the future..."

- **Helmholtz Virtual Institute**

  Microstructure control for thin film solar cells

  * **Cu(In,Ga)Se2 (CIGSe)** absorber layers $\Rightarrow$ efficiencies > 25 %
  * Multi-junctions, concentrator cells based on CIGSe $\Rightarrow$ efficiencies > 30 %
  * **Poly-Si** thin films: **cheap production** of high absorber material quality
  * Microstructural features, defects
    $\Rightarrow$ electrical & optoelectronic properties of CIGSe & Poly-Si
  * Collaboration: Experimental analyses. modeling on scales from subnanometers to cm, numerical simulations

FOCUS: Line-focussed laser- or e-beam induced liquid-phase crystallization

Liquid phase crystallization of silicon

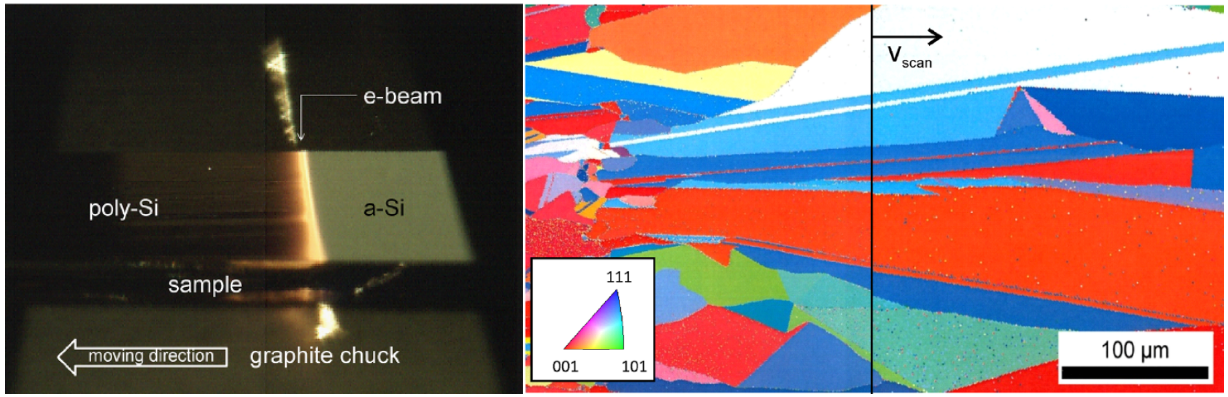

Becker et al., Sol. Energy Mater. Sol. Cells (2013)

Liquid phase crystallization of silicon

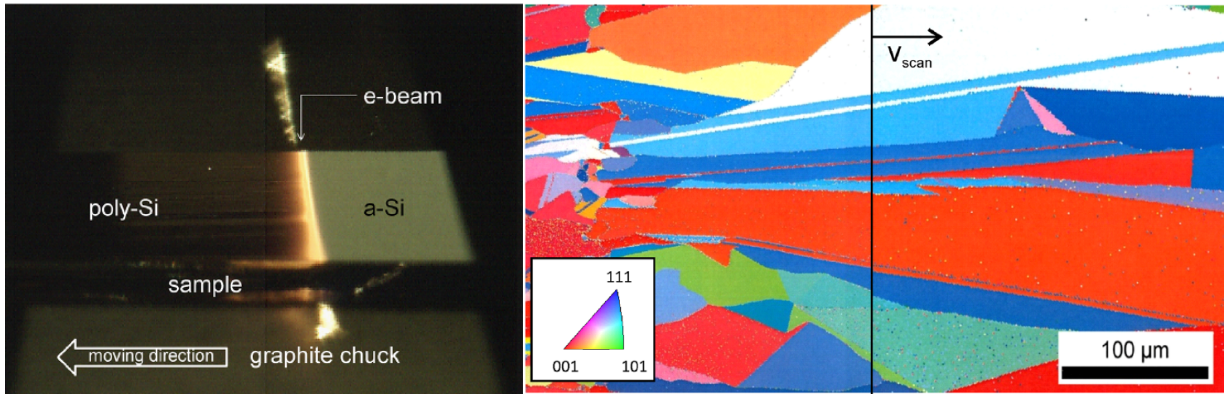

Becker et al., Sol. Energy Mater. Sol. Cells (2013)

- Line-focused electron-beam
- Crystallization exhibit the largest grains & low bulk grain defect density & best electrical material quality
- Cheap large-scale process, **BUT** depends sensitively on the details of grain shapes

Bragard et al., Interf. Sci. (2002), Desai, J. Phys. Chem. Ref. Data (1986), Broughton & Li, Phys. Rev. B (1987), Kobayashi, Physica D (1993), Buta et al., Phys. Rev. E (2007)

Incorporate microscale properties of Si into a phase-field model

Model equation (single 3D grain)

$$\frac{\partial p}{\partial t} = \mathbf{M}(\mathbf{n}, T)\left(\nabla\cdot(\sigma(\mathbf{n})^2\nabla p) + \sum_{i=1}^{3}\partial_{x_i}\left(|\nabla p|^2\sigma(\mathbf{n})\frac{\partial\sigma(\mathbf{n})}{\partial(\partial_{x_i}p)}\right) - \frac{\partial F(p,T)}{\partial p}\right)$$

$\Rightarrow$ Determine $\mathbf{M}(\mathbf{n}, T)$ and $\sigma(\mathbf{n})$ with $\mathbf{n} = \frac{\nabla p}{|\nabla p|}$

from expressions for three crystallographic orientations

- $M_{\{100\}}(T), M_{\{110\}}(T), M_{\{111\}}(T)$
- $\varepsilon_{\{100\}}, \varepsilon_{\{110\}}, \varepsilon_{\{111\}}$

Ansatz: 6-fold anisotropy function:

$$\sigma(\mathbf{n}) = \sigma_0 \left(1 + \delta_1 \sum_{i=1}^{3} n_i^4 + \delta_2 \prod_{i=1}^{3} n_i^2 \right)$$

Determine constants such that:

$$\sigma((1,0,0)) = \varepsilon_{\{100\}}, \quad \sigma((1,1,0)/\sqrt{2}) = \varepsilon_{\{110\}}, \quad \sigma((1,1,1)/\sqrt{3}) = \varepsilon_{\{111\}}$$

Mobility: $$\mathbf{M}(\mathbf{n}, T) = \mathbf{M}_0 \left(1 + m_1(T) \sum_{i=1}^{3} n_i^4 + m_2(T) \prod_{i=1}^{3} n_i^2 \right)$$

with

$$\begin{aligned} \mathbf{M}((1,0,0), T) &= M_{\{100\}}(T) \\ \mathbf{M}((1,1,0)/\sqrt{2}, T) &= M_{\{110\}}(T) \\ \mathbf{M}((1,1,1)/\sqrt{3}, T) &= M_{\{111\}}(T) \end{aligned}$$

$$\frac{\partial p}{\partial t} = M\left[\varepsilon^2 \frac{\partial^2 p}{\partial x^2} - \frac{\partial F}{\partial p}(p,T)\right]$$

- Equilibrium values for the crystalline and liquid phase of Si, at different temperatures[1]
- $C(T)$ for the **crystalline** values at $p = 1$ and
- $L(T)$ for the **liquid** values at $p = 0$

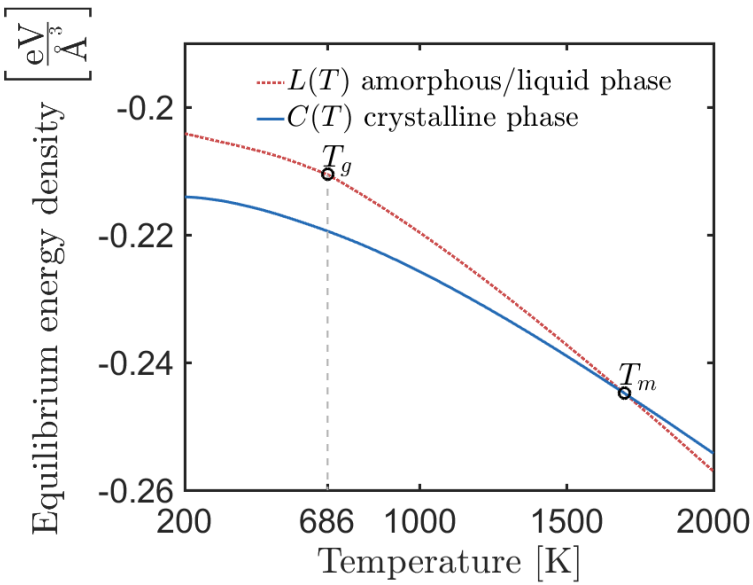

$$F(p,T) = a_0(T) + a_1(T)p + a_2(T)p^2 + a_3(T)p^3 + a_4(T)p^4$$

Fix $a_0(T), \ldots, a_4(T)$ s. t. $(\mathbf{0}, \mathbf{F(0,T)})$ and $(\mathbf{1}, \mathbf{F(1,T)})$ are minima of a double-well potential in p

[2] Based on MD package by S. Ryu and W.Cai, Stanford Univ.

The **bulk free energy** F is modeled as a double well potential in p.

Coefficient ε of the **gradient energy** depends on the interface thickness l.

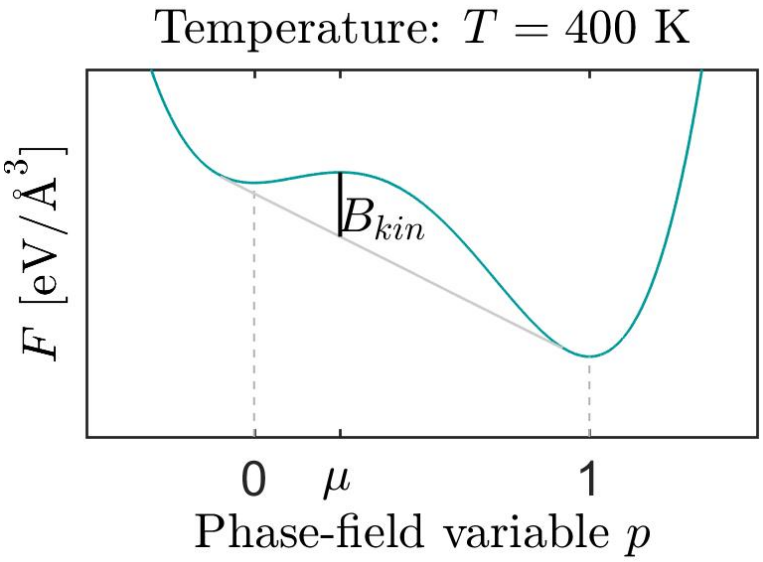

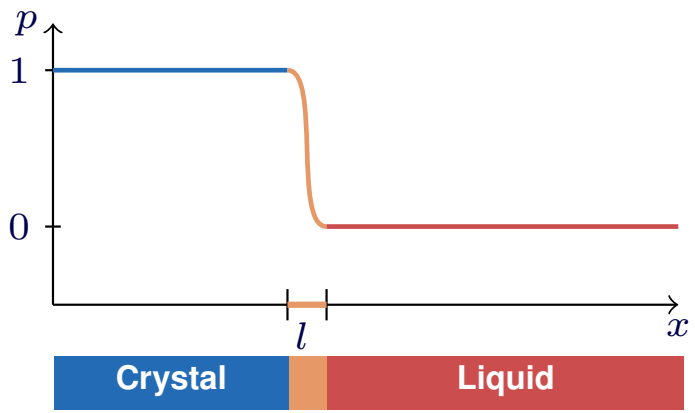

$$\varepsilon = l\sqrt{2B_{kin}}, \quad B_{kin} = \gamma/l$$

- **If we knew interface energy** $\gamma \Rightarrow$ parameters ε and B_{kin} are specified

Experiments show a **Vogel-Fulcher**-type temperature dependence of interface velocity.[2]

$$\nu = const \cdot (T_m - T) \cdot \exp\left(-\frac{B}{T - T_{VF}}\right)$$

Use this in MD simulation using the **Stillinger-Weber potential**.

M is fitted to the MD-calculated velocity and depends on temperature and orientation

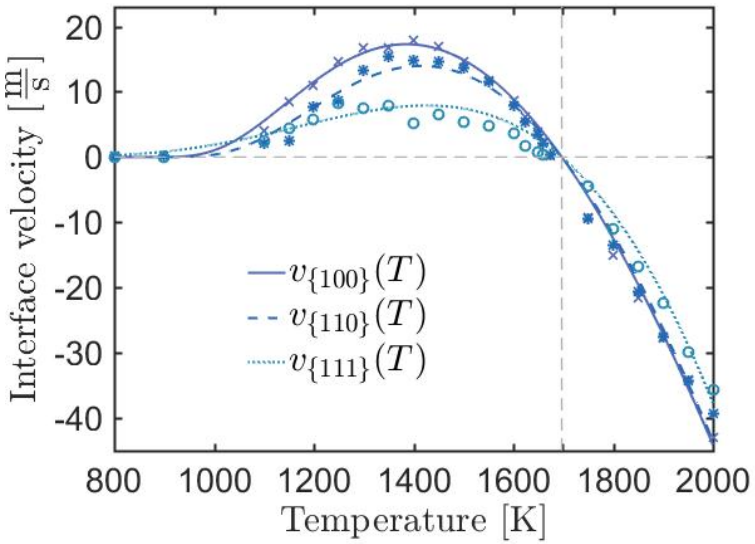

[2] S.R. Stiffler, P.V. Evans, A.L. Greer. Acta metall. mater, 40:1617-1622, 1992

Interface energies

$$\frac{\partial p}{\partial t} = M\left[\varepsilon^2 \frac{\partial^2 p}{\partial x^2} - \frac{\partial F}{\partial p}(p,T)\right],$$

Have: $C(T), L(T)$ $v_{\{100\}}(T), v_{\{110\}}(T), v_{\{111\}}(T)$

Find: $\varepsilon_{\{100\}}, \varepsilon_{\{110\}}, \varepsilon_{\{111\}}$ $F(p,T)$ $M_{\{100\}}(T), M_{\{110\}}(T), M_{\{111\}}(T)$

Need: $\gamma_{\{100\}}, \gamma_{\{110\}}, \gamma_{\{111\}}$

Interface energies

$$\frac{\partial p}{\partial t} = M\left[\varepsilon^2 \frac{\partial^2 p}{\partial x^2} - \frac{\partial F}{\partial p}(p,T)\right],$$

Have: $C(T), L(T)$ $v_{\{100\}}(T), v_{\{110\}}(T), v_{\{111\}}(T)$

Find: $\varepsilon_{\{100\}}, \varepsilon_{\{110\}}, \varepsilon_{\{111\}}$ $F(p,T)$ $M_{\{100\}}(T), M_{\{110\}}(T), M_{\{111\}}(T)$

Need: $\gamma_{\{100\}}, \gamma_{\{110\}}, \gamma_{\{111\}}$

Interface energies

$$\frac{\partial p}{\partial t} = M\left[\varepsilon^2 \frac{\partial^2 p}{\partial x^2} - \frac{\partial F}{\partial p}(p,T)\right],$$

Have: $C(T), L(T)$ $v_{\{100\}}(T), v_{\{110\}}(T), v_{\{111\}}(T)$

Find: $\varepsilon_{\{100\}}, \varepsilon_{\{110\}}, \varepsilon_{\{111\}}$ $F(p,T)$ $M_{\{100\}}(T), M_{\{110\}}(T), M_{\{111\}}(T)$

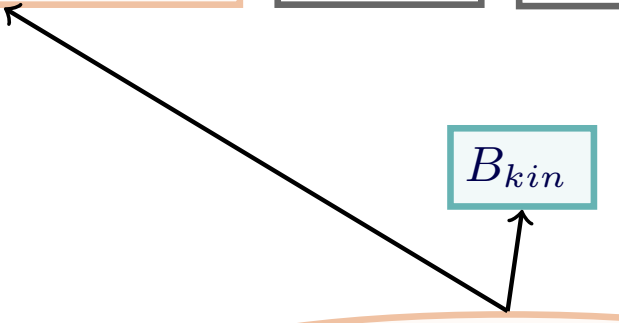

Need: $\gamma_{\{100\}}, \gamma_{\{110\}}, \gamma_{\{111\}}$

Interface energies

$$\frac{\partial p}{\partial t} = M\left[\varepsilon^2 \frac{\partial^2 p}{\partial x^2} - \frac{\partial F}{\partial p}(p,T)\right],$$

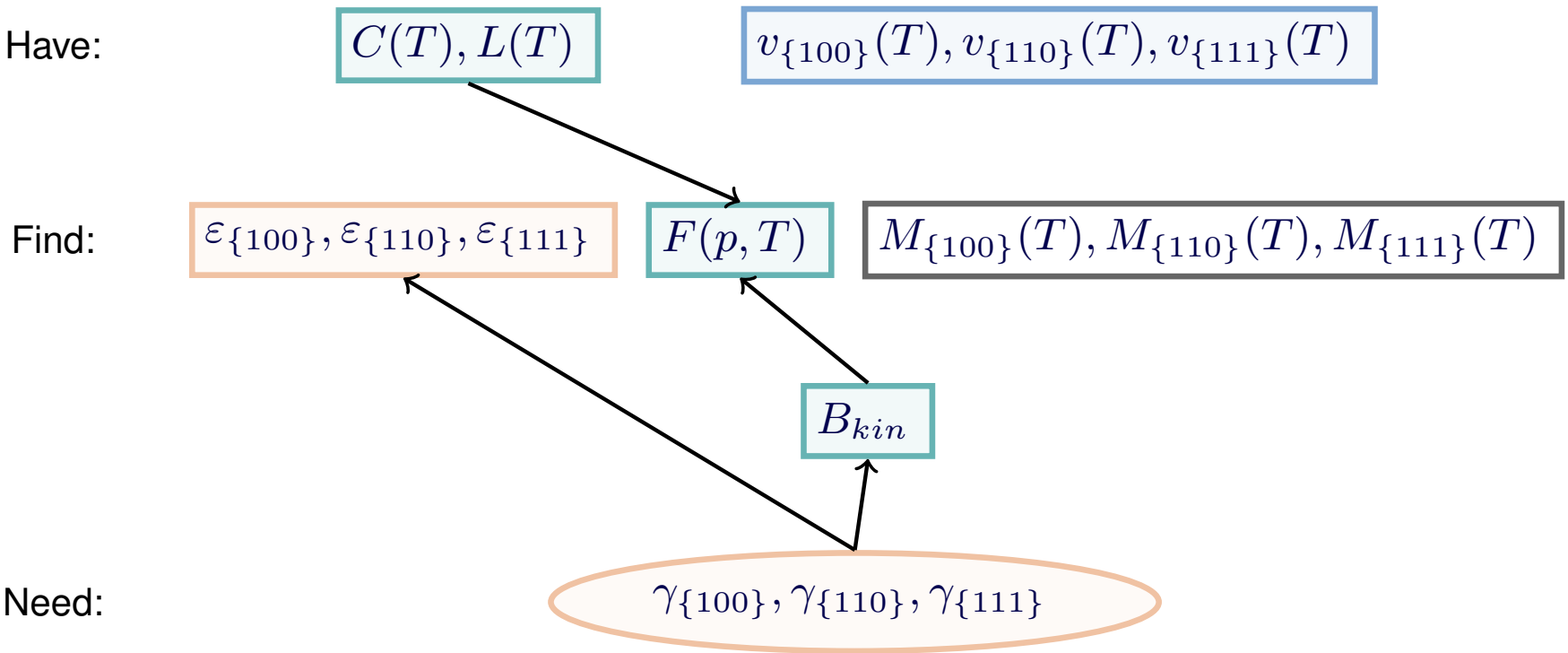

$$\frac{\partial p}{\partial t} = M\left[\varepsilon^2 \frac{\partial^2 p}{\partial x^2} - \frac{\partial F}{\partial p}(p,T)\right],$$

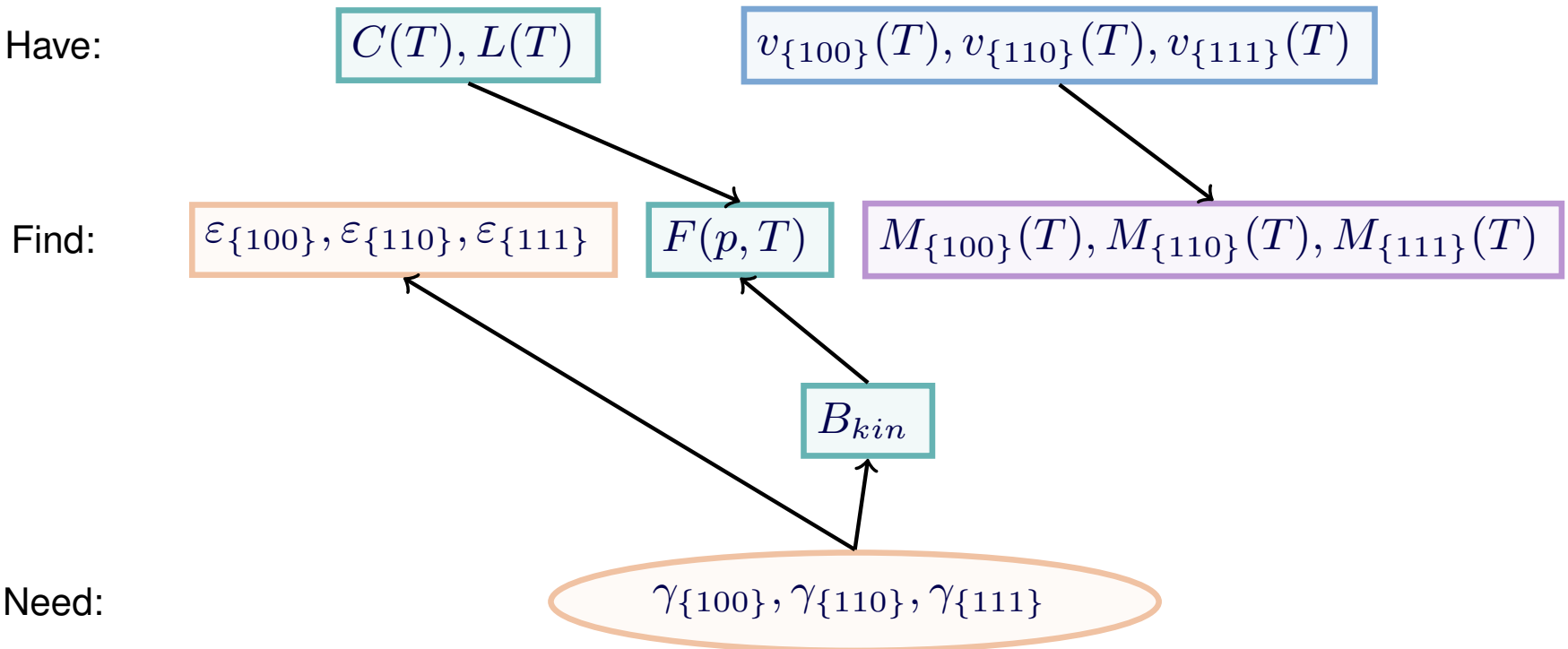

Shape of the grain: 3D Simulations and comparison to experiment

$\gamma_{\{111\}} < \gamma_{\{110\}} < \gamma_{\{100\}}$

- $\gamma_{\{100\}} = 0.0262$ eV/Å^2
- $\gamma_{\{110\}} = 0.0218$ eV/Å^2
- $\gamma_{\{111\}} = 0.0212$ eV/Å^2

$\{110\}$ cut at 44ns

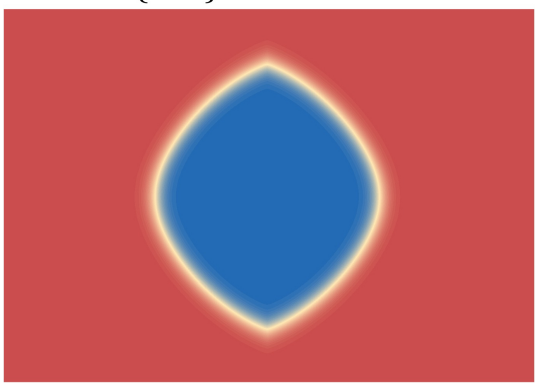

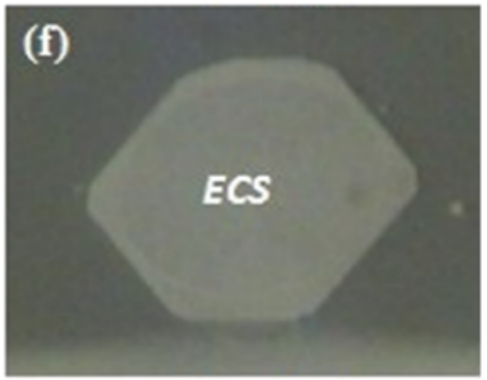

$\gamma_{\{111\}} < \gamma_{\{100\}} < \gamma_{\{110\}}$

- $\gamma_{\{100\}} = 0.0234$ eV/Å^2
- $\gamma_{\{110\}} = 0.0277$ eV/Å^2
- $\gamma_{\{111\}} = 0.0212$ eV/Å^2

$\{110\}$ cut at 44ns

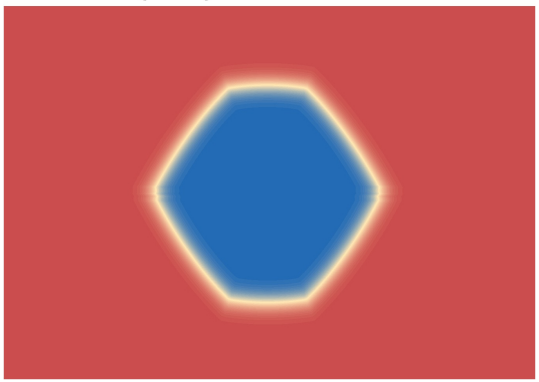

Yang et al., Prog.PV.: Res. App. 2014

Apte & Zeng, Appl. Phys. Lett., (2008), Becker & Hoyt, Phys. Rev. E (2007)

Liquid-phase crystallisation: Ongoing work

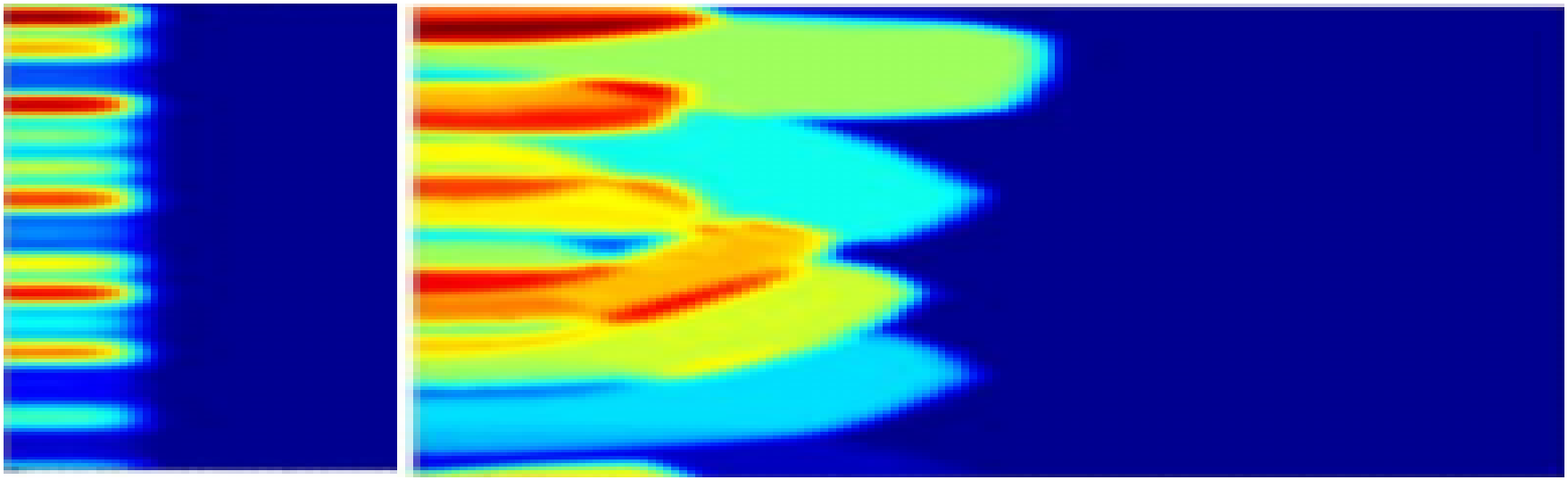

- large scale 3D numerical simulations
- couple to temperature model, defects

  Optimization
  - shape of the temperature profile
  - scanning speeds
  - beam shape

Bergmann, Barragan, Flegel, Albe, W., in: Modelling & Simulation in Mat. Sci. Eng. (2017), Korzec & Wu, DCDS-B (2014)

Light harvesting with 3D Nanostructures: Self-assembly of nanodots

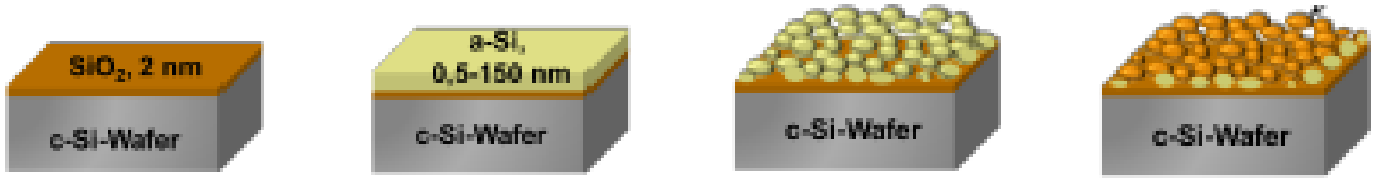

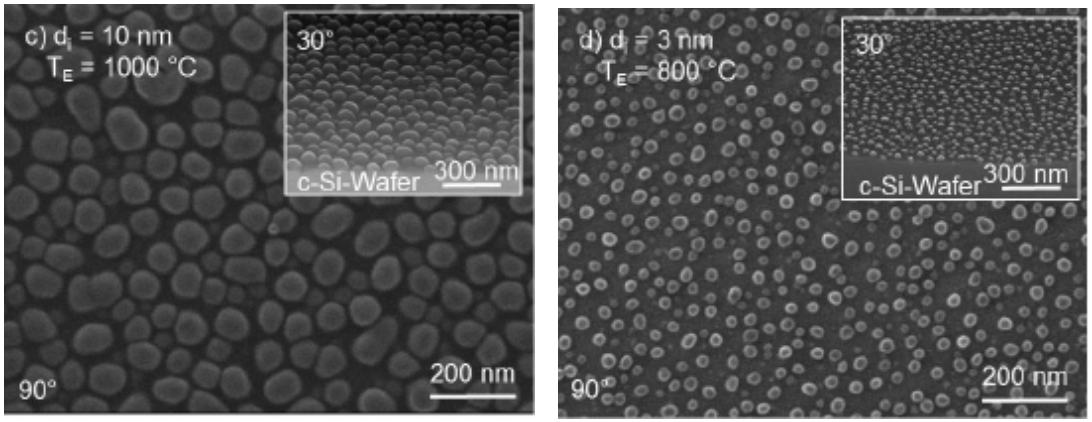

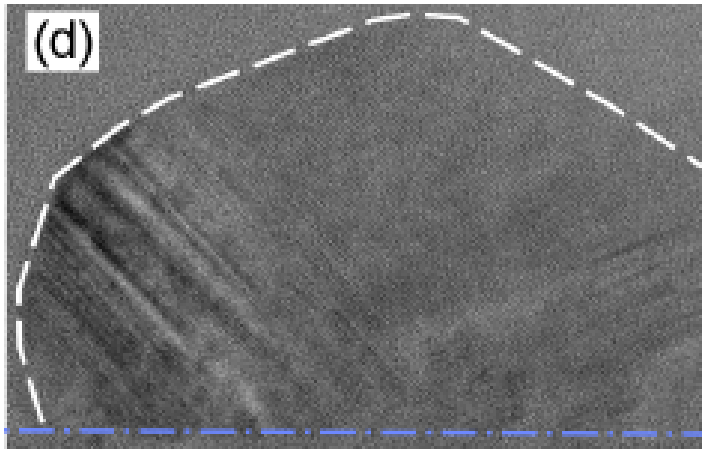

Dr. Maurizio Roczen, Dissertation, TU Berlin 2013

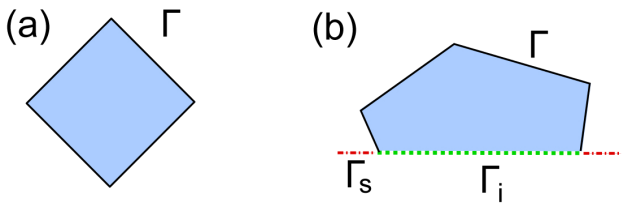

$$\min_{\Omega} \int_{\Gamma} \gamma dS + \int_{\Gamma_i} \gamma_i dS + \int_{\Gamma_s} \gamma_s dS \quad s.t. \quad |\Omega| = \text{const.}$$

$$\Rightarrow \quad \min_{x \in \mathbb{R}^N} f(x) \quad \text{s.t.} \quad c(x) = 0, \quad \text{for} \quad x \geq 0$$

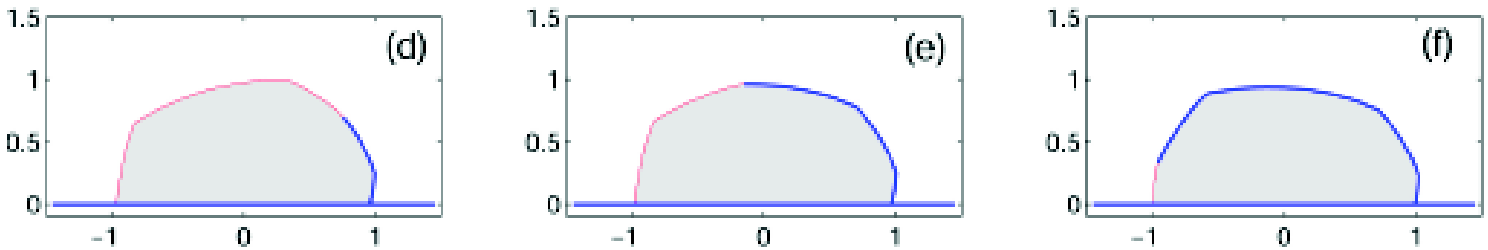

Korzec, Roczen, Schade, W., Rech, J. Appl. Phys. (2014), Winterbottom, Acta Metall. (1967), Eaglesham, PRL (1993)

Sharp-interface model

$$V_n = \frac{\partial^2 \mu}{\partial s^2} = \frac{\partial^2}{\partial s^2}\left[\gamma(\theta) + \gamma''(\theta)\right]\kappa$$

At x_c :

No flux $\quad 0 = \frac{\partial}{\partial s}\left[\gamma(\theta) + \gamma''(\theta)\right]\kappa$

Young-Herring $\quad \gamma(\theta)\cos\alpha - \gamma'(\theta)\sin\alpha = \frac{\sigma_{FS} - \sigma_{VS}}{\lambda_m}$

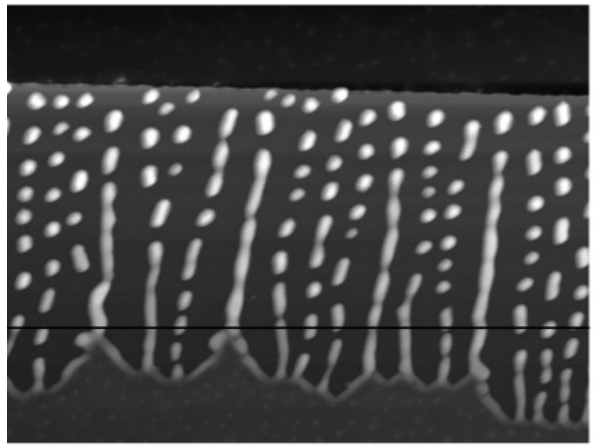

Leroy et al. Phys.Rev.B (2012)

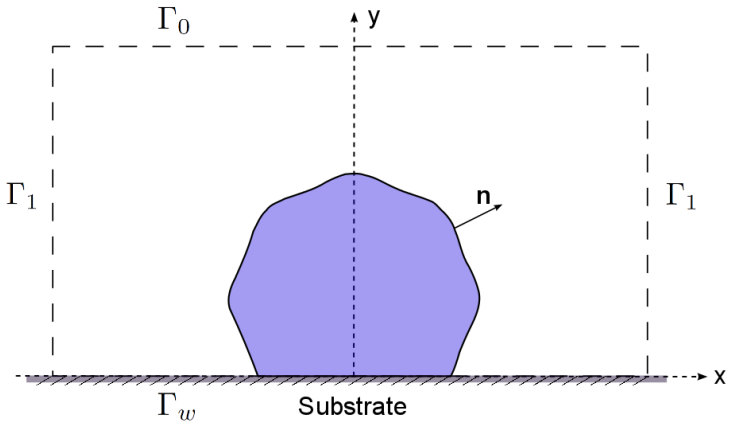

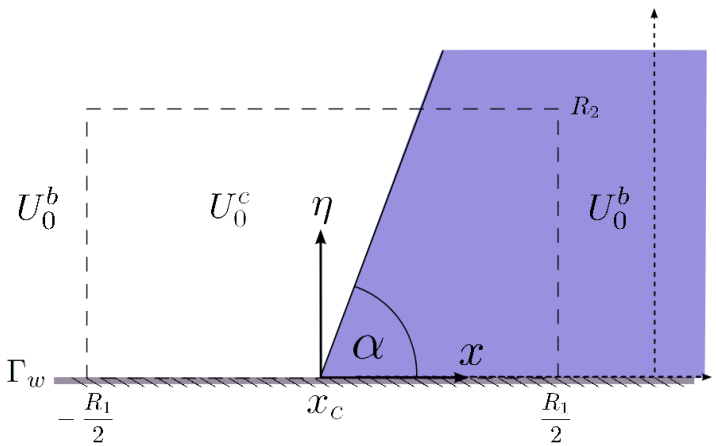

Cahn & Taylor, Acta Metall. Mater. (1994), Thompson, Annu. Rev. Mater. Res. (2012), Danielson et al. J. App. Phys. (2006), Pierre-Louis et al., Eur. Phys J. (2010), Wang et al., Phys. Rev. B (2014), Leroy et al., Surf. Sci. Rep. (2016)

Free Energy $W = \int_\Omega f_{FV}\, d\Omega + \int_{\Gamma_w} f_w\, d\Gamma$

$$f_{FV} = \lambda_m \left(F(u) + \frac{\varepsilon^2}{2} |\nabla u| \right) \qquad f_w = \frac{\sigma_{VS} + \sigma_{FS}}{2} - \frac{u(3-u^2)}{4}(\sigma_{VS} - \sigma_{FS}).$$

Phase-field $\varepsilon^2 \partial_\tau u = \nabla \cdot m(u) \nabla \mu \qquad \mu = F'(u) - \epsilon^2 \nabla \left(\gamma\gamma' \begin{pmatrix} -u_y \\ u_x \end{pmatrix} + \gamma^2 \nabla u \right)$

Boundary conditions

On Γ_w: $\mathbf{n}_\Omega \cdot (m(u)\nabla\mu) = 0 \qquad \varepsilon\, \mathbf{n}_\Omega \cdot \left[\gamma(\theta)\gamma'(\theta) \begin{pmatrix} -u_y \\ u_x \end{pmatrix} + \gamma(\theta)^2 \nabla u \right] + \frac{f_w'}{\lambda_m} = 0$

On $\Gamma_0 \cup \Gamma_1$: $\mathbf{n}_\Omega \cdot (m(u)\nabla\mu) = 0 \qquad \mathbf{n}_\Omega \cdot \nabla u = 0$

With $F(u) = \frac{1}{2}(1-u^2)^2$ and $\mathbf{m(u) = (1-u^2)^2}$

Anisotropic phase-field model for solid dewetting

* Matched asymptotics yields a sharp interface model governed by surface diffusion
* Matching involves two interior layers $\Rightarrow$ and exponential asymptotics
* Dynamics of triple-points uses multiple inner layers to obtain the Young-Herring condition and the contact angle

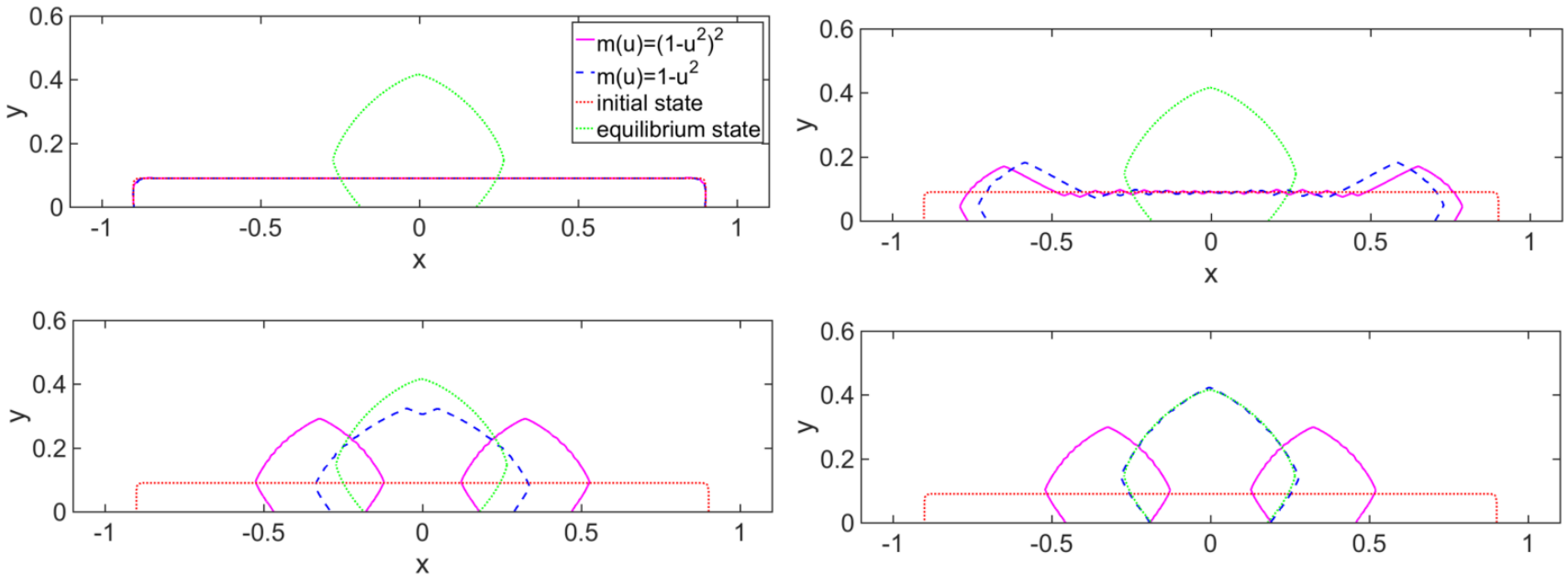

Phase field model: Isotropic case $u \in [1, -1]$

$$u_t = \nabla \cdot \left[(1-u^2)^2 \nabla \mu\right], \qquad \mu = -\varepsilon^2 \nabla^2 u + f'(u),$$
$$f(u) = (1-u^2)^2$$

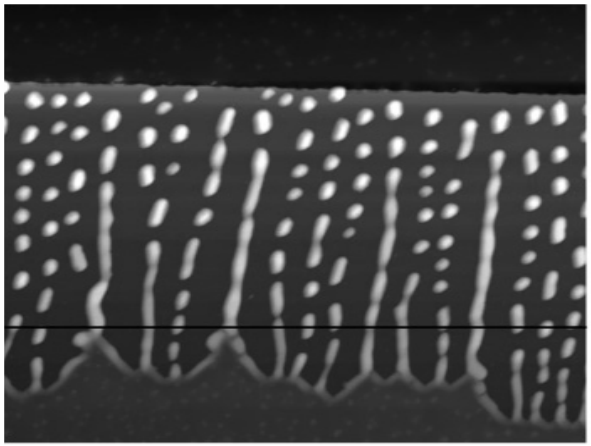

Sharp interface limit: $\varepsilon \to 0 \qquad v_n = \Delta_\Gamma \kappa$

Thin film approximation: $h_t + \Delta^2 h = 0,$

A note on the instability: n < 3

$$h_t + \nabla \cdot (h^n \nabla \Delta h) = 0$$
$$h \to 1 \quad \text{for} \quad x \to \infty$$
$$h = 0,\ \nabla h \cdot n_s = 1,\ h^n (\nabla \Delta h) \cdot n_s = 0 \text{ at } x = s(y,t)$$

Three scenarios for the base states

- $n = 0$ finite time rupture
- $3/2 < n < 3$ no finite time rupture
- $0 < n < 3/2$ unknown

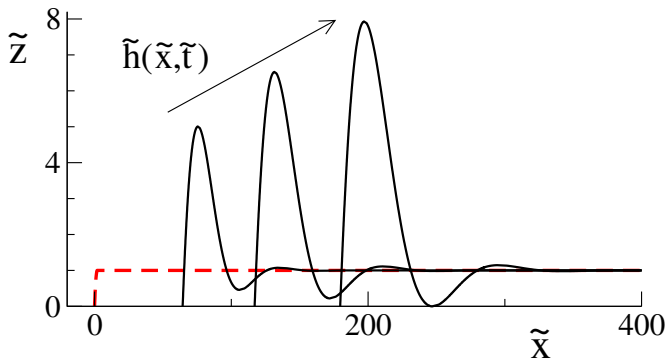

King & Bowen, EJAM (2001), Wong et al., Acta Mater. (2000), Dziwnik, Münch, W., Nonlinearity, (2017), Dziwnik, Jachalski WIAS preprint 2332

Other structuring mechanisms: Self-assembly of quantum dots

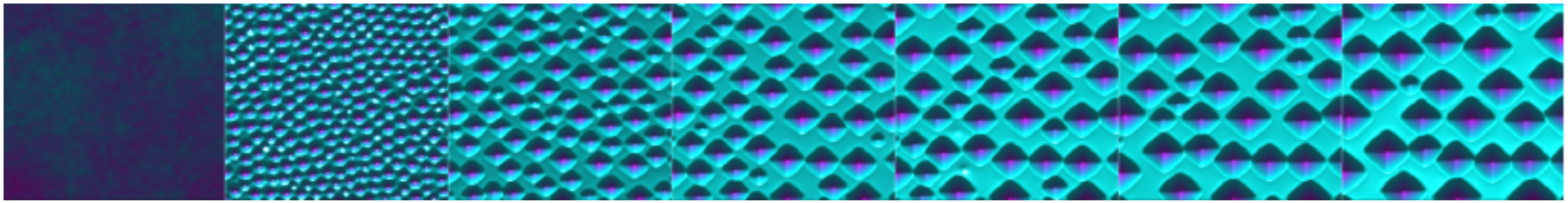

Stranski-Krastanov growth

Mullins' surface diffusion formula

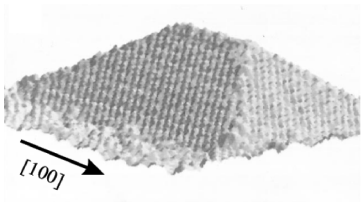

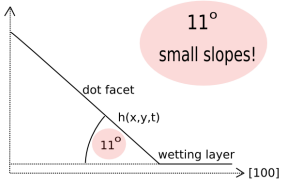

$$h_t = \sqrt{1 + |\nabla h|^2}\, \mathcal{D}\, \nabla_s^2 \mu$$

$$\mathcal{F} = \mathcal{F}_{sed} + \mathcal{F}_{\kappa} + \mathcal{F}_{wet} + \mathcal{F}_{anis} + f$$

C. Teichert et al., Appl. Phys. A (1998)

$$\alpha = \frac{\mathbf{H}}{\mathbf{L}} \ll \mathbf{O(1)}$$

6^{th} (- 4^{th}) - Order Convective Cahn-Hilliard equations

Asaro, Tiller, Metall. Trans (1972), Grinfeld, Sov. Phys. Dokl. (1987), Spencer, Voorhees, Davis, J Appl Phys (1993), Tersoff et al., PRL (2002), Golovin et al., Phys. Rev. B (2004), Korzec,Evans,Münch,W., SIAM J. Appl. Math.(2008), Khenner,Tekalgin,Levine EPL (2011), Korzec, Nayar, Rybka, J. Dyn. Diff. Equ. (2016)

Organic solar cells: Polymer blends

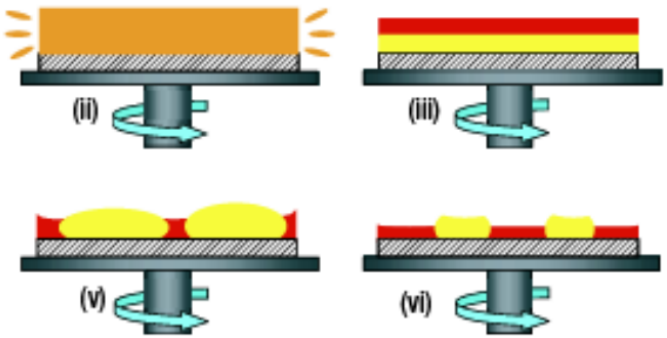

Heriot & Jones 2005, Xu & Wang (2011)

Donor and acceptor polymers with defined grade of demixing

⇒ Self-organization during layer evaporation

Heterojunction polymer cell: photons generates **excitons**

Solar cell performance

* Exciton and charge transport in bulk
* Exciton dissociation at donor-acceptor interface

Exciton and charge carrier **diffusion length of few 10nm**

⇒ optimize the absorber morphology

⇒ **highly folded heterojunction**

with controlled morphology

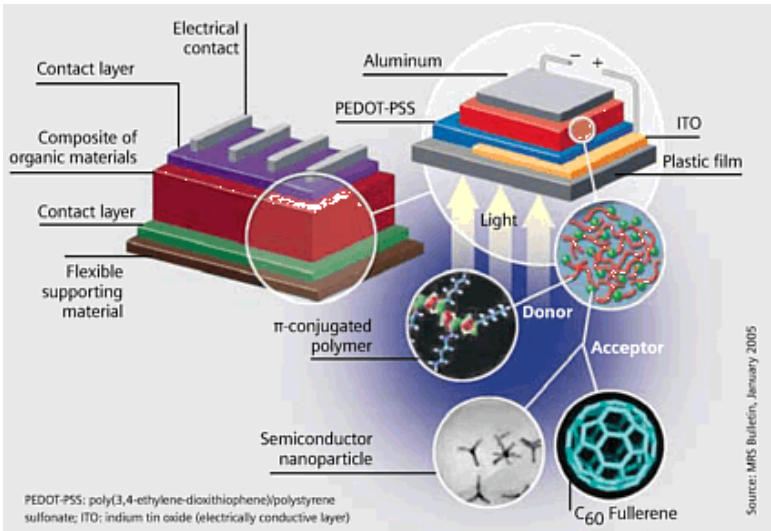

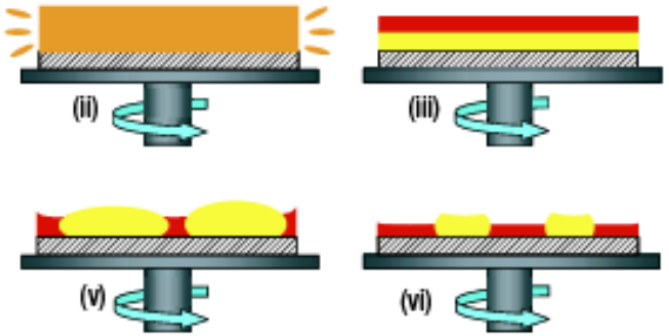

Heriot & Jones 2005, Xu & Wang (2011)

Donor and acceptor polymers with defined grade of demixing

⇒ Self-organization during layer evaporation

Heterojunction polymer cell: photons generates **excitons**

Solar cell performance

* Exciton and charge transport in bulk
* Exciton dissociation at donor-acceptor interface

Exciton and charge carrier **diffusion length of few 10nm**

⇒ optimize the absorber morphology

⇒ **highly folded heterojunction**

with controlled morphology

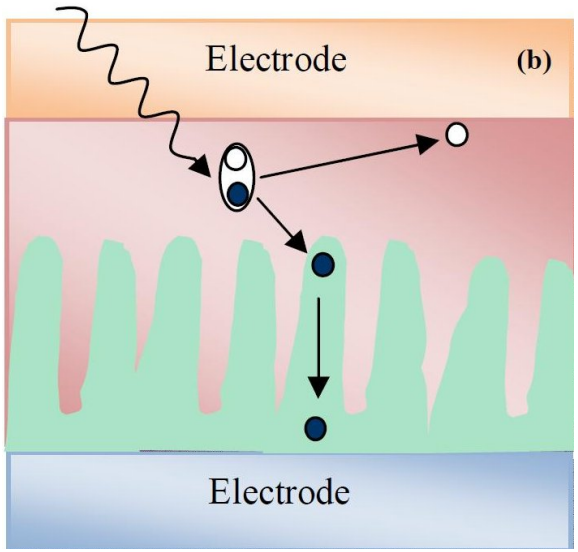

Transitions in morphology:

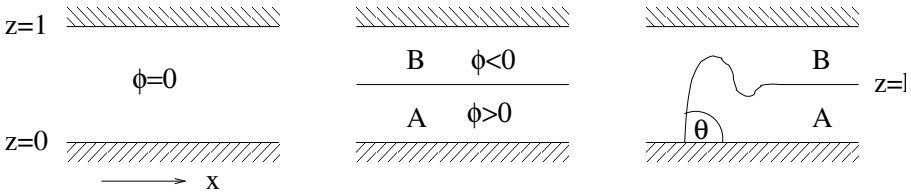

ϕ order parameter, μ chemical potential,

F bulk free energy

$$\phi_t = \Delta\mu, \qquad \mu = F'(\phi) - \varepsilon^2\Delta\phi,$$

$$F(\phi) = -\phi^2/2 + \phi^4/4,$$

Assume antisymmetric walls at $z = 0, 1$:

$$\mu_z = 0 \quad \text{(no-flux)},$$

$$\varepsilon\phi_z = \beta_1(1 - \phi^2)$$

Surface directed spinodal decomposition

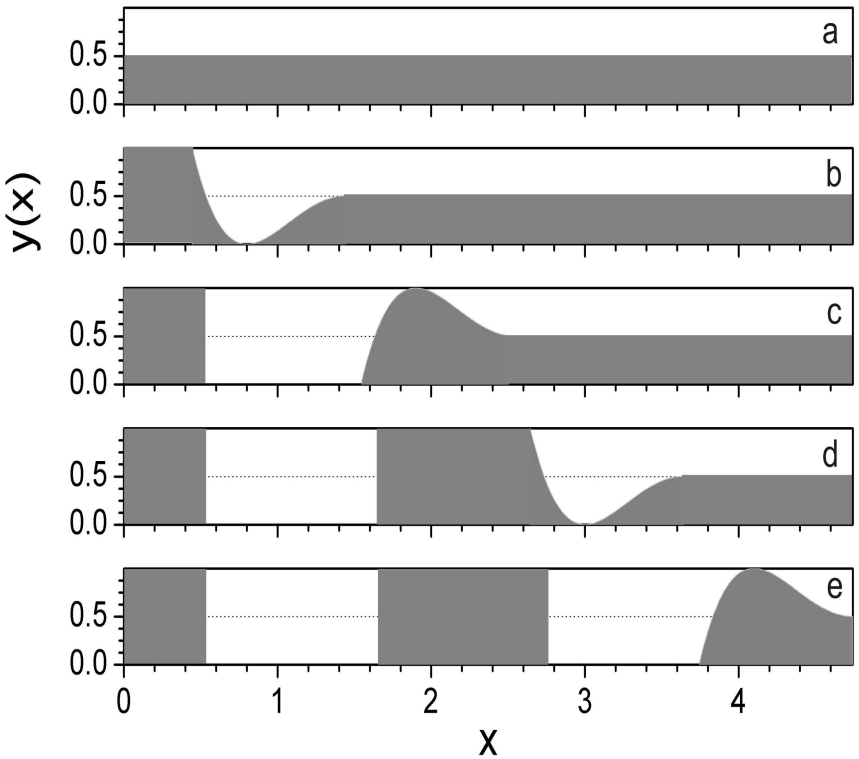

Jaczewska et al., Macromolecules (2008), Dunbar et al., Phys. J. E Soft Matter (2010), Buxton and Clarke, Europhys. Lett. (2007), Wodo et al., Appl. Phys. Lett. (2014)

Sharp-interface model

$$\Delta \mu_1 = 0 \quad \text{for } 0 < z < 1,\ z \neq h,$$
$$\partial_z \mu_1 = 0 \qquad \text{at } z = 0,\ 1,$$
$$\mu_1 = \sigma\kappa \qquad \text{at } z = h,$$
$$h_t = -\frac{\nabla \mu_1 \cdot (-h_x, 1)}{2}\Big|_-^+ \qquad \text{at } z = h,$$

At the 3-phase contact-line:

$$h = 0, \quad h_x = \tan\theta, \quad q = \partial_x \int_0^1 \mu \, dz = 0$$

with $\cos\theta = \frac{2\beta_1}{3\sigma}$ (Cahn 77 - Modica 87)

At $x \to \infty$: $h \to 1, \quad q \to 0$

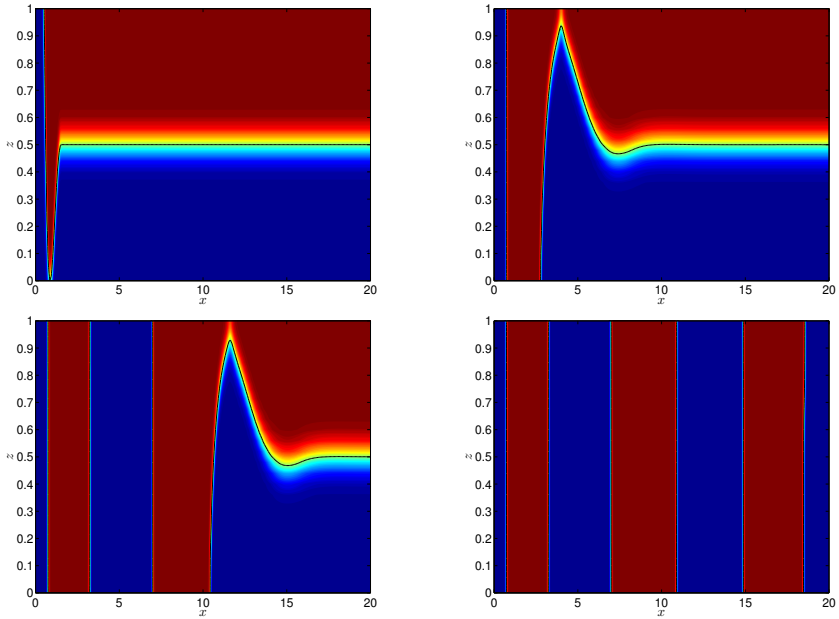

No/weak surface energy: $\theta = 85^\circ$, $\varepsilon = 0.03$, $\beta_1 = 0.03$. Solution shown at times $t = 0$, $t = 165$, $t = 498$ and final state

Thin film approximation

$$h_t + h_{xxxx} = 0, \qquad (n = 0)$$
$$x = s(t): \quad h = 0, \quad h_x = 1, \quad h_{xxx} = 0;$$
$$x \to \infty: \quad h \to 1, \quad h_{xxx} \to 0.$$

Puri & Binder (2007), Gheoghegan & Krausch (2003), Xu & Wang 2011, Hennessey et al. 2014, 2015

- **Rechargeable batteries, hydroelectric power, solarfuels**

- **Rechargeable batteries, hydroelectric power, solarfuels**

LITHIUM ION BATTERIES

Phyisco-chemical phenomena

- Ion diffusion in electrolytes
- Lithium intercalation of electrodes
- Surface and transfer reactions
- Electrochemical double layers
- Many particle electrodes

Battery management

- Assessment of State of Health (SOH)
- ageing of battery

Further problems

- Online assessment of SOH: faster than real time simulations for e-vehicles
- **2nd life batteries**: Recycle automobile batteries for large scale stationary storage systems

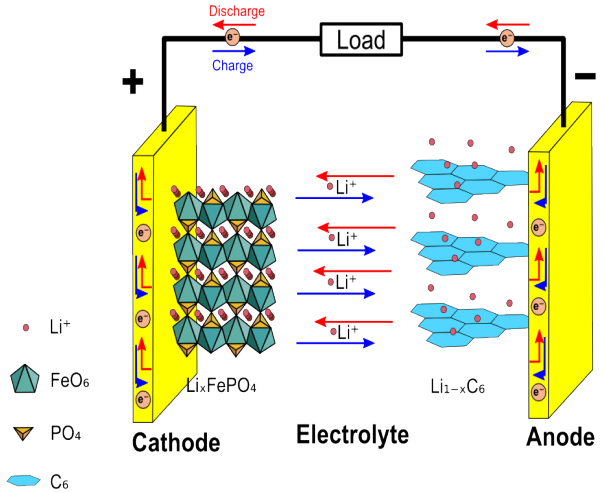

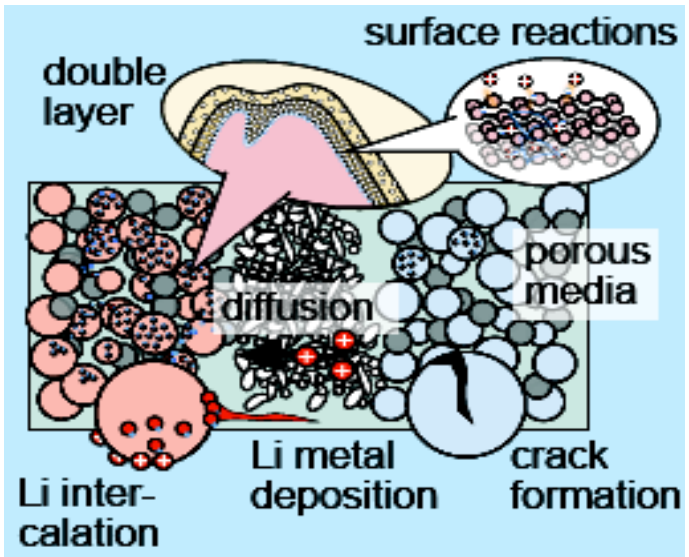

Phase Transition in $LiFePO_4$ (Weichert et al. 2012)

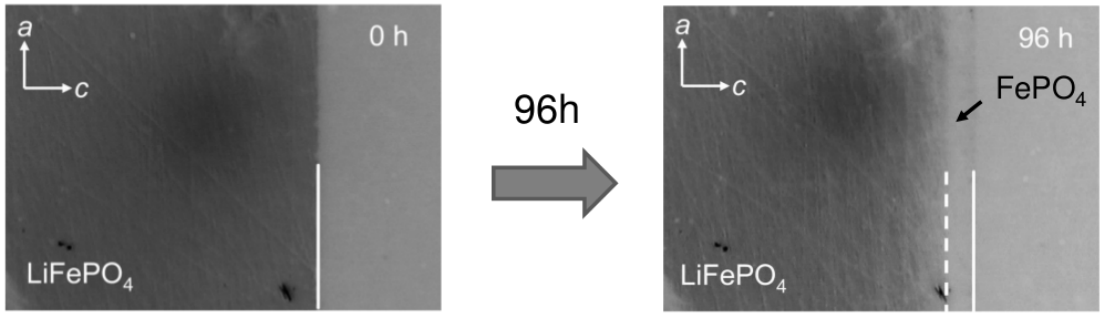

- $LiFePO_4$ undergoes a phase transition. Changes in volume 6.8%.

2-Phase Lithiation in a-Si (Wang et al. 2013)

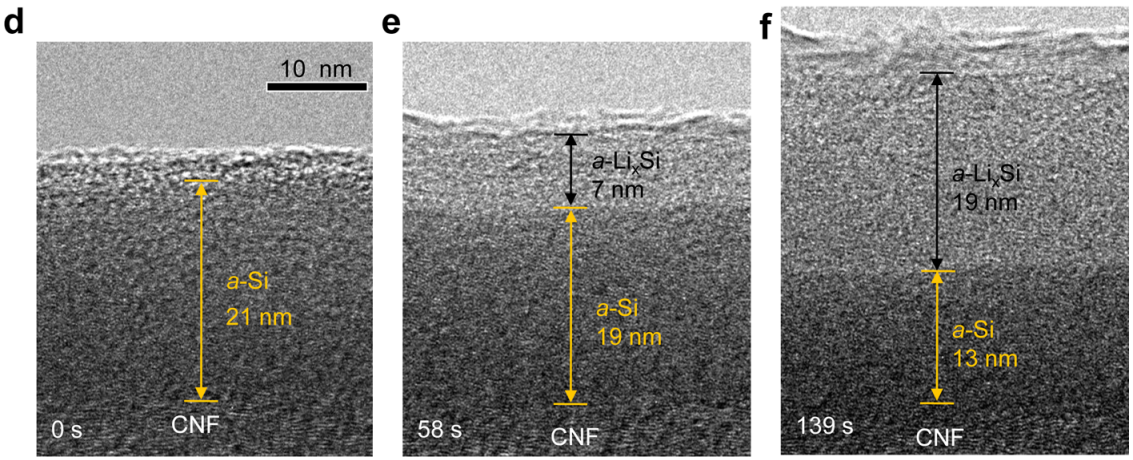

- c-Si and a-Si undergo two-phase lithiation. Si changes in volume 300%. Si has a huge specific charge, 4200 $mAhg^{-1}$ compared to graphite, 372 $mAhg^{-1}$

Cogswell, Bazant, Nano (2012), Cubuk, Kaxiras, Nano Lett (2014), Levitas et al., J. Mech. Phys. Solids (2016),

Stress curve for a thin layer electrode (Sethuraman et al 2010):

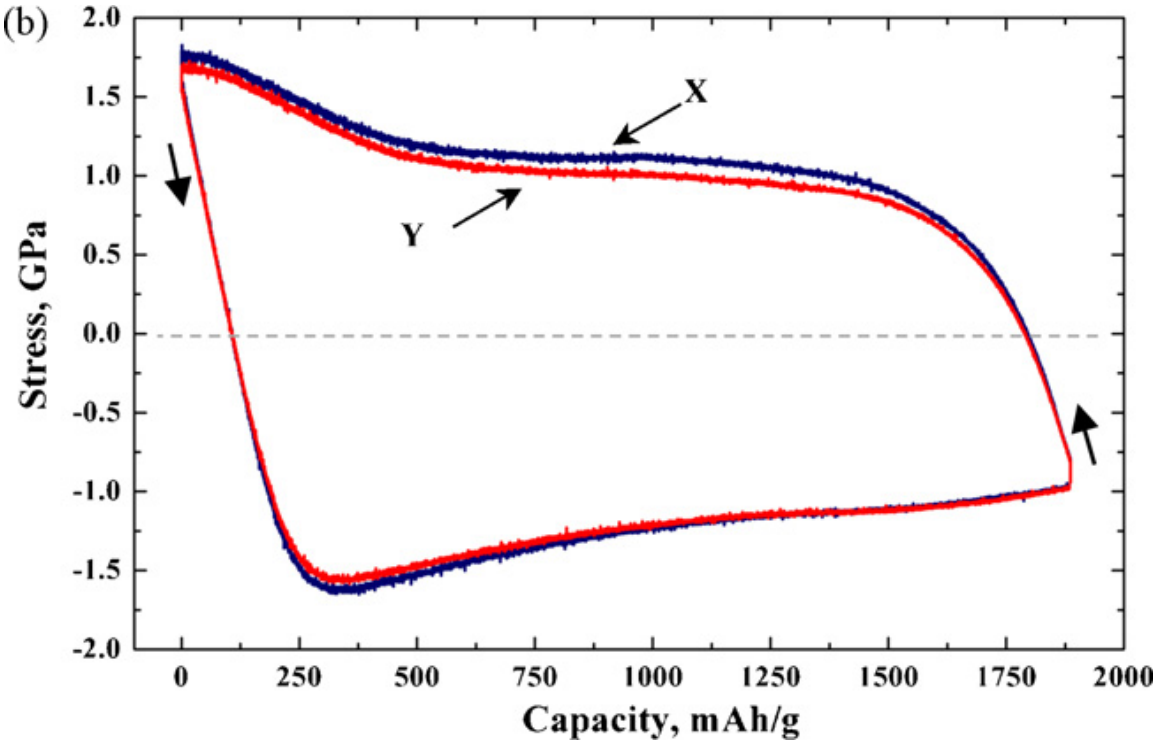

- Zhao et al. (2012), Pharr et al. (2014) based on yield stress.
  The yield stress does not reach the theoretical value.
- **What would the effect of a phase transition be?**

Simplified experimental set-up

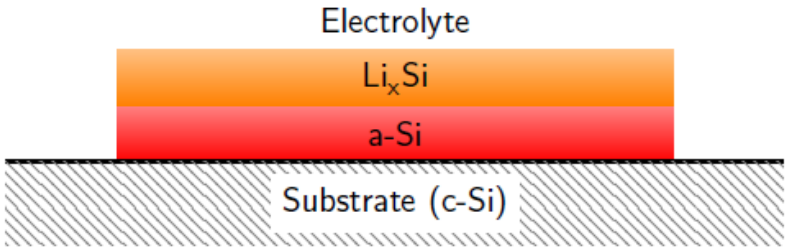

$$c_t = \nabla \cdot (M(c)\nabla\mu)$$
$$\mu = -\Delta c + W_c^{\mathrm{ch}}(c) + W_c^{\mathrm{el}}(e(u), c) + \nu c_t$$
$$0 = \mathrm{div}(W_e^{\mathrm{el}}(e(u), c))$$

* c vector of concentrations, u displacement field
* The elastic energy W^{el} will in general be nonlinear, anisotropic
* $M(c)$ mobility matrix, in general anisotropic.
* νc_t is the viscous term, ν could depend on c too.
* Y reaction term, general nonlinear function $R(c, \mu)$

Boundary conditions

Electrolyte

$$\sigma \cdot n = 0$$
$$n \cdot \nabla c = 0$$
$$n \cdot \nabla \mu = Y.$$

Substrate

$$u = 0$$
$$n \cdot \nabla c = 0$$
$$n \cdot \nabla \mu = 0.$$

Simplified experimental set-up

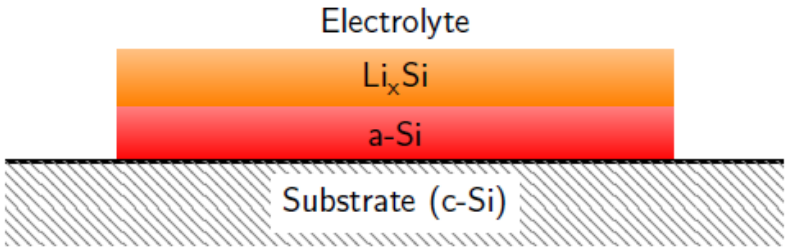

$$c_t = \nabla \cdot (M(c)\nabla\mu)$$
$$\mu = -\Delta c + W_c^{\mathrm{ch}}(c) + W_c^{\mathrm{el}}(e(u), c) + \nu c_t$$
$$0 = \mathrm{div}(W_e^{\mathrm{el}}(e(u), c))$$

Boundary conditions

Electrolyte

$$\sigma \cdot n = 0$$
$$n \cdot \nabla c = 0$$
$$n \cdot \nabla \mu = Y.$$

Substrate

$$u = 0$$
$$n \cdot \nabla c = 0$$
$$n \cdot \nabla \mu = 0.$$

* Assume constant flux boundary conditions, isotropic mobility and elasticity, concentration dependent elastic constants and eigenstrain
* Numerical method: finite volume with an adaptive nonlinear multigrid algorithm (S. Wise et al 2007).

Lithium-ion intercalation: Comparison to experiment

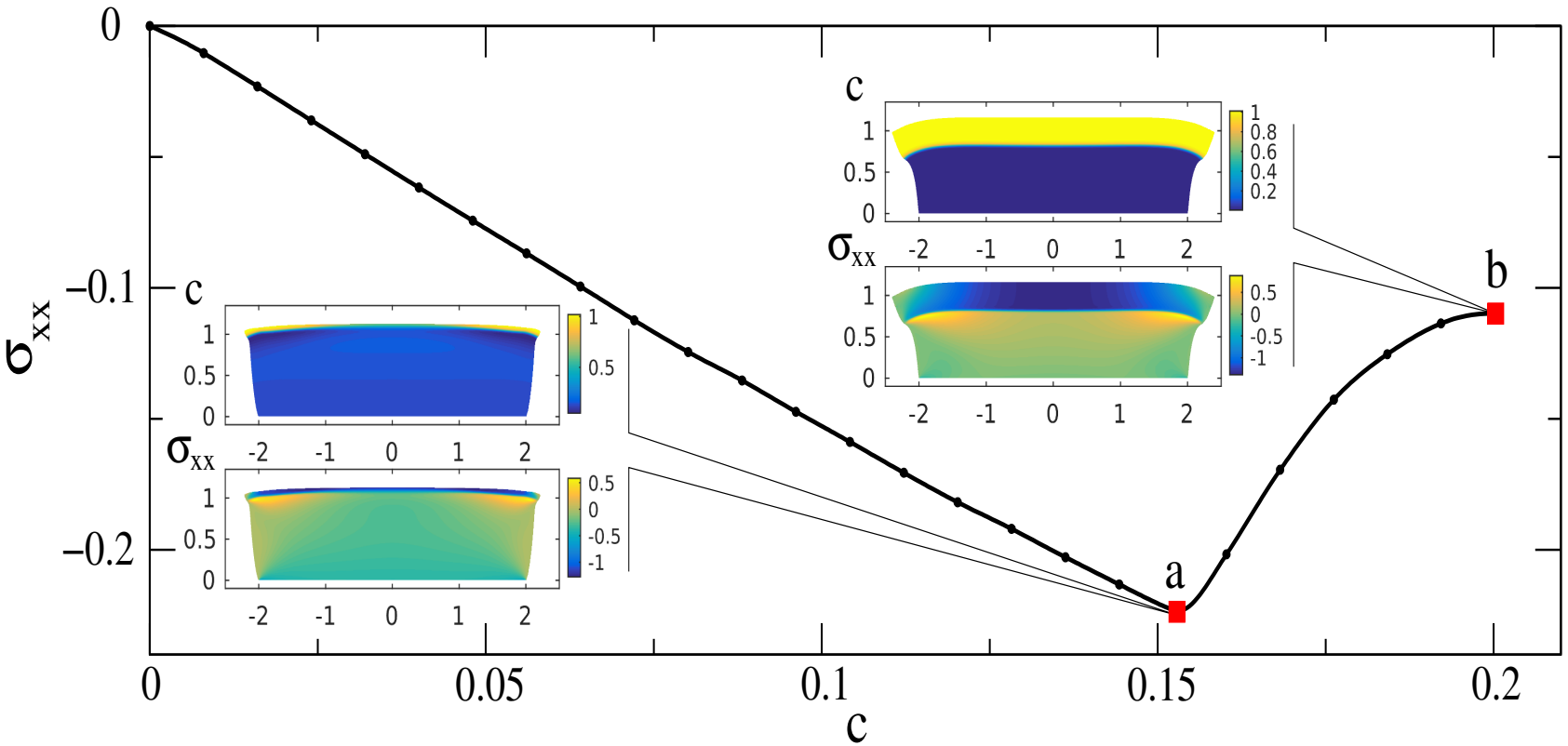

Sethuraman et al. (2010), Meca, Münch, W., PRS A (2016), EJAM (2017)

Lithium-ion intercalation: An instability

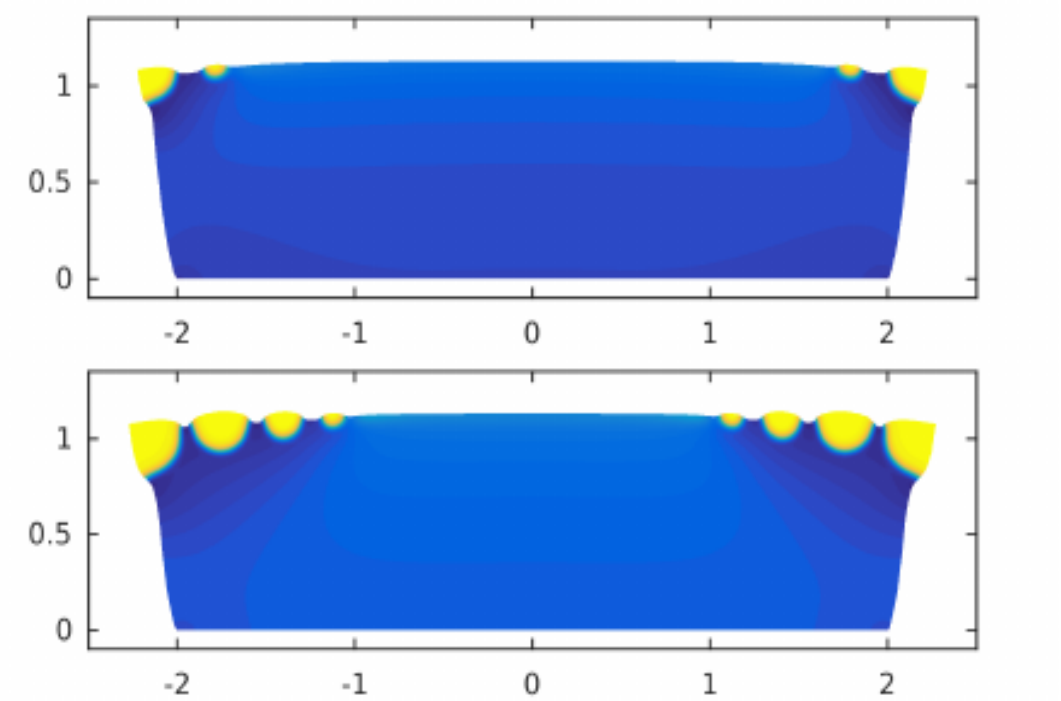

Meca, Münch, W., WIAS preprint 2387 (2017), Kraus, Roggensack, WIAS preprint 2231 (2016)

Sibylle Bergmann (TU Berlin/WIAS)

Karsten Albe (TU Darmstadt)

Daniel Barragan (TU Darmstadt)

Daniel Abou-Ras (HZB)

Bernd Rech (HZB)

Maurizio Roczen (HZB)

Marion Dziwnik (TU Berlin/WIAS)

Maciek Korzek (WIAS/TU Berlin)

Matt Hennessy (U. Oxford)

Viktor Burlakov (U. Oxford)

Alain Goriely (U. Oxford)

Esteban Meca (WIAS)

Andreas Münch (U. Oxford)

...